1-1-2014

Development And Evaluation Of Plga-S-S-Peg Micelles Coencapsulating Curcumin Difluorinated And Paclitaxel For Synergistic Therapeutic Efficacy

Lakshmi Deepika Cheemalakonda
Wayne State University,

DEVELOPMENT AND EVALUATION OF PLGA-S-S-PEG MICELLES COENCAPSULATING CURCUMIN DIFLUORINATED AND PACLITAXEL FOR SYNERGISTIC THERAPEUTIC EFFICACY

by

LAKSHMI DEEPIKA CHEEMALAKONDA

THESIS

Submitted to the Graduate School

of Wayne State University,

Detroit, Michigan

in partial fulfillment of the requirements

for the degree of

MASTER OF SCIENCE

2014

MAJOR: PHARMACEUTICALSCIENCES

(Pharmaceutics)

Approved By:

_____

Advisor Date

DEDICATION

Dedicated to my loving daughter Aditi and my family

ACKNOWLEDGEMENTS

It is with a profound sense of gratitude that I thank Dr. Joshua Reineke, my advisor. His mentorship and encouragement have taught me to think independently and strive for scientific excellence. I thank Dr. Reineke, for everything I learnt from him with regards to science and research. I will ever be indebted to you for all I learnt from you directly and indirectly.To my committee members, Dr. Guangzhao Mao, Dr. Fei Chen and Dr. Olivia Merkel, thank you for your critical analysis, suggestions and advice. Your critical evaluation of my work had only made it better and put me through a process of learning and taught me how to take criticism and address it. Thank you all for investing so much of your precious time. I would like to thank all my lab members for their suggestions and help regarding my research. I would also like to thank Avinash for providing help with some experiments. I would thank our postdoctoral fellow Dr. Cheng and under graduate Dina for helping with my cell culture work. I would also thank Dr. Shiv for his help with N.M.R and providing his valuable inputs regarding the synthesis of conjugates. Last but not the least, I would love to thank my loving daughter for allowing to spend more time on studies and my husband for his constant support throughout my studies. I would like to respectfully express my deepest appreciation and gratitude to my loving

parents and my brother. Their limitless love, support, and patience have been a source of strength throughout my endeavors. Their innumerable sacrifices throughout my life have been instrumental in carrying me to this point in my academic endeavor. I owe every one of my achievements and successes to my family. I would never ever have been able to achieve what I did in my life if it was not for their love, care, sacrifice, and unflinching support in times of great adversity and otherwise. Finally, it goes without saying that if it was not for the special mercy of the almighty I would not have accomplished anything ever.

TABLE OF CONTENTS

Acknowledgements iii

List of tables viii

List of figures ix

List of abbrevations xi

Chapter 1 - Introduction 1

1.1 Cancer 1

1.2 Curcumin 7

1.2.1 Origin 7

1.2.2 Mechanism of action 9

1.2.3 Curcumin as chemosensitizer 11

1.2.4 Pharmacokinetics of curcumin 12

1.3 Difluorinated curcumin (CDF) 14

1.3.1 Origin and mechanism of action 14

1.3.2 Pharmacokinetic analysis 15

1.4 Polymeric micelles 16

1.4.1 Advantages of micelles 18

1.5 testing the chemosensitizing ability of CDF 20

1.5.1 Paclitaxel, origin and mechanism of action 20

1.5.2 Possible mechanism of synergy between CDF and paclitaxel....22

Chapter 2 – Hypothesis and specific aims 25

2.1 Hypothesis.....25

2.2 Specific aims.....25

Chapter 3 – Materials and methods 1

3.1 Materials.....27

3.2 Methods.....28

3.2.1 fabrication of micelles encapsulatinf CDF, paclitaxel and coencapsulating both CDF and paclitaxel 28

3.2.1.1 Synthesis of PEG-S-S-PLGA-CDF.....28

3.2.1.2 Characterization of conjugates.....30

3.2.1.3 Preparation of CDF-PLGA-S-S-PEG micelles coencapsulating CDF and/or paclitaxel.....31

3.2.2 Morphological and physicochemical characterization of micelles 32

3.2.2.1 Percentage drug loading and percentage encapsulation efficiency for micelles 32

3.2.2.2 Micelle size and zeta potential 33

3.2.2.3 critical micelle concentration (CMC) determination.....33

3.2.3 In vitro drug release studies.....35

3.2.4 Cell culture studies 35

3.2.4.1 In vitro cytotoxicity studies 35

3.2.4.2 Evaluation of combination effect of CDF and paclitaxel 37

Chapter 4 – Results and discussion 42

4.1 Characterization of conjugates 42

4.2 Physicochemical characterization of micelles 44

4.2.1 Drug loading and encapsulation efficiency for micelles 44

4.2.2 Micelle size and zeta potential 44

4.2.3 Critical micelle concentration 45

4.2.4 In vitro drug study of micelles 46

4.2.5 Cell culture studies 44

4.2.5.1 In vitro cytotoxicity studies 48

4.2.5.2 Evaluation of combination effect of CDF and paclitaxel in micelles 53

Chapter 5 – Conclusions and future directions 72

References 75

Abstract 85

Autobiographical statement 88

LIST OF TABLES

Table 1: Standard graph of CDF in acetone by U.V/Visible spectrophotometry at wavelength 355 nm 40

Table 2: Standard graph of paclitaxel in acetonitrile by HPLC at wavelength 225 nm 41

Table 3: Drug loading, encapsulation efficiency, size and zeta potential measurements of micelle formulations 44

Table 4: 50 % inhibitory concentration values (IC_{50}) of CDF and paclitaxel alone and in combination on BXPC3 cells, in the free drug form and micelle formulation.....69

Table 5: 50 % inhibitory concentration values of CDF and paclitaxel alone and in combination on SKOV3 cells, in the free drug form and micelle formulation 69

Table 6: CDF and paclitaxel combination index (CI) against SKOV3 cells CI < 1, synergistic; CI = 1, additive; CI > 1, antagonistic. 70

Table 7: CDF and paclitaxel combination index (CI) against BXPC3 cells CI < 1, synergistic; CI = 1, additive; CI > 1, antagonistic 70

Table 8: Dose reduction index (DRI) values for CDF and paclitaxel with micelles coencapsulating both CDF and paclitaxel when compared to CDF micelles and paclitaxel micelles in BXPC3 and SKOV3 cell lines at 72 h time point. 71

LIST OF FIGURES

FIGURE 1: Cell-cell interactions and ECM deposition contributing to desmoplasia in pancreatic cancer 4

FIGURE 2: Chemical structure of curcuminoids.....8

FIGURE 3: Modulation of multiple molecular targets by curcumin in cancer cells. Arrows represent induction/activation whereas blunt-ended lines represented inhibition/repression 10

FIGURE 4: Structure of Difluorinated curcumin 14

FIGURE 5: Design of a polymeric micelle carrier system 16

FIGURE 6: CDF-PLGA conjugate formation 29

FIGURE 7: PEG-SS-NH_2 and CDF-PLGA-SS-PEG formation.....30

FIGURE 8: FTIR spectra of synthesized conjugates.....57

FIGURE 9: AFM images of CDF-PLGA-SS-PEG micelles with conjugate concentration of 1 mg/ml 58

FIGURE 10: AFM images of CDF-PLGA-SS-PEG micelles with conjugate concentration of 100 µg/ml 58

FIGURE 11: CMC for PLGA-SS-PEG micelles using pyrene as a fluorescence probe 59

FIGURE 12: Invitro drug release studies of micelle coencapsulating CDF and paclitaxel in PBS and PBS containing 20 µM, 20 mM and 5 mM GSH 60

FIGURE 13: % Cell viability of BXPC3 cells upon incubation with free CDF and micelles encapsulating CDF at the end of 24 h, 48 h and 72 h 61

FIGURE 14: % Cell viability of BXPC3 cells upon incubation with free Paclitaxel and micelles encapsulating Paclitaxel at the end of 24 h, 48 h and 72 h 62

FIGURE 15: % Cell viability of BXPC3 cells upon incubation with free CDF and Paclitaxel and micelles encapsulating both CDF & Paclitaxel at the end of 24 h, 48 h and 72 h 63

FIGURE 16: % Cell viability of BXPC3 cells upon incubation with control micelles at the same dilutions as micelles with drug at the end of 24 h, 48 h and 72 h 64

FIGURE 17: % Cell viability of SKOV3 cells upon incubation with free CDF and micelles encapsulating CDF at the end of 24 h, 48 h and 72 h 65

FIGURE 18: % Cell viability of SKOV3 cells upon incubation with free Paclitaxel and micelles encapsulating Paclitaxel at the end of 24 h, 48 h and 72 h 66

FIGURE 19: % Cell viability of SKOV3 cells upon incubation with free CDF and paclitaxel and micelles encapsulating both CDF & Paclitaxel at the end of 24 h, 48 h and 72 h 67

FIGURE 20: % Cell viability of SKOV3 cells upon incubation with control micelles at the same dilutions as micelles with drug at the end of 24 h, 48 h and 72 h 68

LIST OF ABBREVATIONS

TGFβ	Transforming growth factor β
FGF2	Fibroblast growth factor
CTGF	Connective tissue growth factor
IL-1β	Interleukin-1β
ECM	Extra cellular matrix
PDGF	Platelet-derived growth factor
NF-κB	Nuclear factor kappa B
EGFR	Epidermal growth factor receptor
HER2	Human epidermal growth factor receptor
5-LOX	5-lipoxygenase
iNOS	Inducible nitric oxide synthase
IKK	I-Kappa B kinase
CDF	Difluorinated curcumin
5-FU	5-Fluoro uracil
CMC	Critical micelle concentration
MPS	Mono nuclear phagocytic system
PEG	Polyethylene glycol
EPR	Extra permeation and retention
MDR	Multi drug resistance

P-gp	P-Glyco protein
PLGA	Poly (D,L-lactide-co-glycolide)
DCC	N, N' – Dicyclohexyl carbodiimide
DMAP	2-Dimethil amino pyridine
NHS	N-Hydroxy succinimide
GSH	Glutathione
MTT	3-(4,5-Dimethylthiazolyl-2)-2,5-diphenyl tetrazolium bromide
OD	Optical density
IC_{50}	Half maximal inhibitory concentration
CI	Combination index
DRI	Dose reduction index

CHAPTER 1: INTRODUCTION

1.1 CANCER

The simplest definition according to American cancer society [1], cancer is a group of diseases characterized by uncontrollable growth and spread of abnormal cells. If the spread is not controlled it could result in death of patient. Cancer is the second leading cause of death in united states and currently one in four deaths are due to cancer [3]. Cancer cells are formed due to certain abnormalities in the normal cells and they would divide uncontrollably even in presence of signals that normally would inhibit cell growth. Cancer cell properties are abnormality, uncontrollability and invasiveness. They divide in an uncontrollable manner and pileup into a non-structured mass or tumor. Tumors are said to be benign if they remain at their origin and considered malignant if they invade into other parts of the body [4, 5]. Tumors are solids or non-solid depending on the body part they grow. More than 80% of tumors are solid tumors and most common sites are breast, pancreas, ovarian, lungs, prostate and colon etc. Non-solid tumors usually form in blood like leukemia and lymphoma and circulate around the body through the blood stream.

PANCREATIC CANCER

There have been several advancements in cancer therapy from past 4 decades in all areas of cancer. However there was not much improvement in 5 year survival rate of pancreatic cancer (3% in 1975 and 6% in 2011) [3]. Pancreatic cancer is the most aggressive form of human cancer and only about 10% of the cases have tumor just confined to pancreatic region at the time of diagnosis [6]. The overall 5-year survival rate is lowest for pancreatic cancer (3-5%) of all major cancers. Surgery is an option for treatment in very few pancreatic cancer patients and it would only improve the survival rate up to 10 – 15%. In USA pancreatic cancer is the 4^{th} leading cause of cancer deaths [6]. Metastatic pancreatic cancer survival rate is 3-5 months without active treatment, 6-10 months for locally advanced disease and which could improve to 11-15 months with surgical resection. Because of the aggressive nature of the tumor, only for minority of patients (10-15%) can potentially undergo curative surgery [7]. The 5-year survival rate of pancreatic cancer is very low (20%) when compared to staging cohorts who has other cancers such as breast (98%) and colon (90%). So improved pancreatic cancer therapies are needed [3]. Pancreatic ductal adenocarcinoma is a solid tumor which forms a dense desmoplastic

layer around the tumor cells and this poses as a main barrier for any drug delivery systems to reach the cells

The main pathological condition in pancreatic cancer is the formation of dense desmoplastic layer surrounding the tumor cells. The word Desmoplasia is derived from the greek words desmos meaning “band” or “fastening” and plassein meaning to “mold” or “form”. Desmoplastic reaction involves overproduction of extracellular matrix proteins and extensive proliferation of myofibroblast-like cells [1]. This dense connective tissue will contain cellular components like stellate cells and extra cellular matrix proteins like collagen types i, iii, iv, fibronectin, laminin, hyaluronan and glycoprotein osteonectin. Desmoplasia reduces the elasticity of the tumor and thereby increases the interstitial pressure which inturn will decrease the rate of perfusion of chemotherapeutic agents in tumor cells and causes reduction in efficacy of the drugs **(figure 1)**. Desmoplasia is the major contributing factors for developing chemoresistance in pancreatic cancer [1, 8]. Transforming growth factor β (TGFβ), basic fibroblast growth factor (FGF2) connective tissue growth factor (CTGF), and interleukin-1β (IL-1β) stimulates ECM production whereas platelet-derived growth factor (PDGF) stimulates the proliferation of the myofibroblast-like cell population.

All these cellular and non-cellular components contribute to pathogenesis of pancreatic cancer [1, 9].

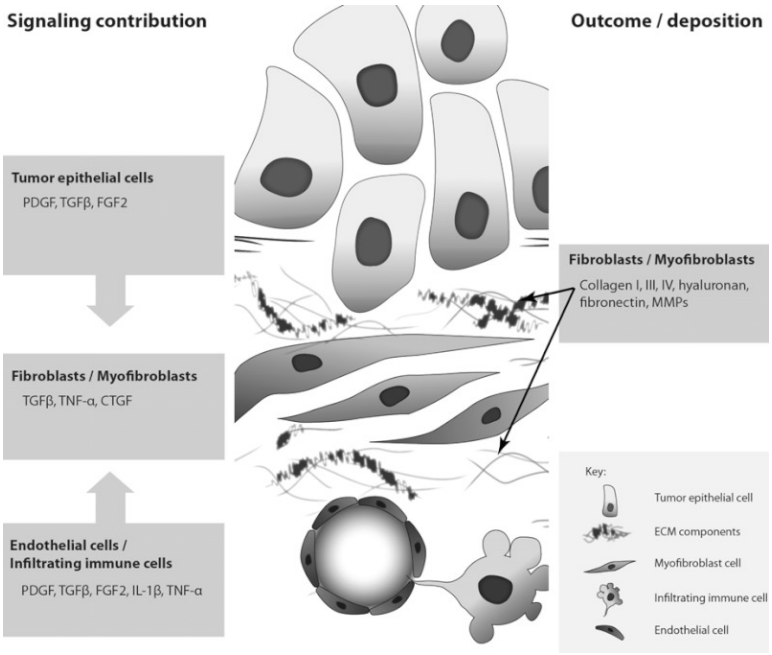

FIG 1: Cell-cell interactions and ECM deposition contributing to desmoplasia in pancreatic cancer[2]

Currently the only curative treatment for pancreatic cancer is surgical resection and only about 15% of the cases detected were still in surgically resectable stage [10]. Surgical resection increases the survival rate to 15-25% [11]. Chemotherapy remains the frontline approach to pancreatic cancer with FOLFOX (oxaliplatin and 5-fluorouracil) or Abraxane (albumin-bound paclitaxel) and gemcitabine being the standard-of-care treatment modalities. Achieving higher drug concentration in tumor cells without affecting the normal cells is the primary goal for any cancer chemotherapy.

Drug resistance often limits the success of chemotherapy. Many new chemotherapeutic approaches to pancreatic cancer are currently in clinical trials, including FOLFOX-6 (FOLFOX and folinic acid), FOLFOX-A (FOLFOX, luecovorin, and Abraxane), and numerous hedgehog inhibitors with gemcitabine. In advanced pancreatic cancer these approaches are further complicated by desmoplastic tumor properties[8]. Pancreatic cancer often develops drug resistance both by intrinsic and acquired mechanisms [12]. Resistance to gemcitabine therapy often limits the success of chemotherapy [13]. Cisplatin has been shown to work in gemcitabine resistant tumor however cisplatin resistance will be developed shortly after the commencement of treatment [14]. Chemoresistance can develop by multiple mechanisms. Biological chemoresistance could arise mainly due to the development of resistance to drug uptake, altered sensitivity of intended targets for the drug and increased efflux of the drug. Whereas physiological chemoresistance can occur because of the poor tissue vasculature which increases the interstitial pressure as well as increases production of extra cellular matrix proteins due to desmoplastic reaction [1]. Therefore, several concurrent approaches are important in pancreatic cancer, including targeting the tumor, penetrating the fibrotic capsule, localizing the release of chemotherapeutics and using multi-target

therapies (to overcome drug resistance).

1.2 CURCUMIN

1.2.1 ORIGIN

Curcumin (1,7-bis(4-hydroxy 3-methoxy phenyl)-1,6- heptadiene-3,5-dione), a polyphenol, is a natural compound that is derived from turmeric, the powdered rhizome of the medicinal plant *Curcuma longa Linn [15]*. It is called turmeric in English, haldi in hindi and ukon in Japanese and it has been used in Asian medicine since the second millenium BC. Curcumin has been used as aromatic spice and coloring agent in Asian cooking. Curcumin has also been recognized in traditional indian medicine for treatment of various respiratory conditions like asthma, bronchial hyperactivity, allergy as well as anorexia, sinusitis and hepatic disease [16, 17]. In addition to this, curcumin, along with other natural substances like slaked lime, has been used topically for wounds and inflammation. The phytochemical curcumin consists of various curcuminoids like curcumin I (or curcumin, ≈77%), curcumin II (demethoxycurcumin, ≈17%) and curcumin III (bisdemethoxycurcumin, ≈3%)[16] **(figure 2).**

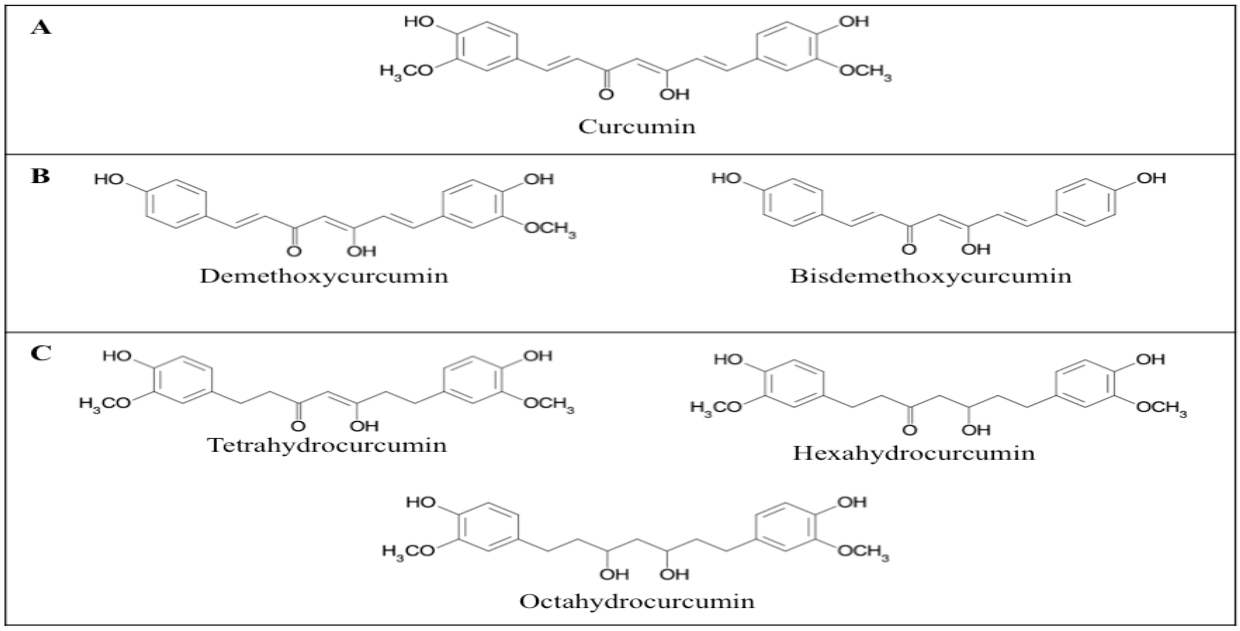

FIG 2: Chemical structure of curcuminoids [18]

By the observation of multiple advantages of naturally occurring compounds in traditional medicine, researchers have further evaluated their studies on these compounds towards their anti-tumor efficacy. Curcumin, was found to have broad range of activity because of its ability to affect multiple intra cellular targets [19]. Several studies done on curcumin over the past decade has proven its profound activity as anti-inflammatory [20], antioxidant [21], anticarcinogenic [22], hepatoprotective [23], thrombosuppressive [24], cardioprotective [25], antiarthritic [26], and anti-infectious [27] properties. To date, there were no reports of curcumin toxicity on either animal or human study [16]. It was found to be safe at even high dose of 8 grams/day during human trials and this makes it a

desirable candidate for cancer therapy along with reduction of the cytotoxicity to the normal cells [28, 29].

1.2.2 MECHANISM OF ACTION

Curcumin affects all three stages of carcinogenesis: initiation, promotion and progression **(figure 3).** Curcumin exerts its action mainly by inhibition of transcription factor nuclear factor kappa B (NF-κB), Ap-1, β–catenin, epidermal growth factor receptor (EGFR), human epidermal growth factor receptor (HER2), and STAT-3. It also affects various oxygenases, such as COX-2 and 5-lipoxygenase (5-LOX), inducible nitric oxide synthase (iNOS), cell cycle proteins (cyclin Dl and p21), cytokines (TNF, IL-1, IL-6, chemokines), as well as cell surface adhesion molecules and thereby affects several proinflammatory pathways [18, 30]. COX-2 is over expressed in many varieties of malignancies including pancreatic cancer. COX-2 mediated prostaglandin synthesis promotes the growth of tumor cells as well as COX-2 over expression inhibits apoptosis. This COX-2 expression is regulated by NF-κB and curcumin was shown to inactivavte NF-κB. This proves that curcumin is effective in pancreatic cancer therapy [31]. Because of the ability of curcumin to affect different molecular mechanisms in cancer without much toxicity it is a very desirable candidate

for cancer therapy and further research.

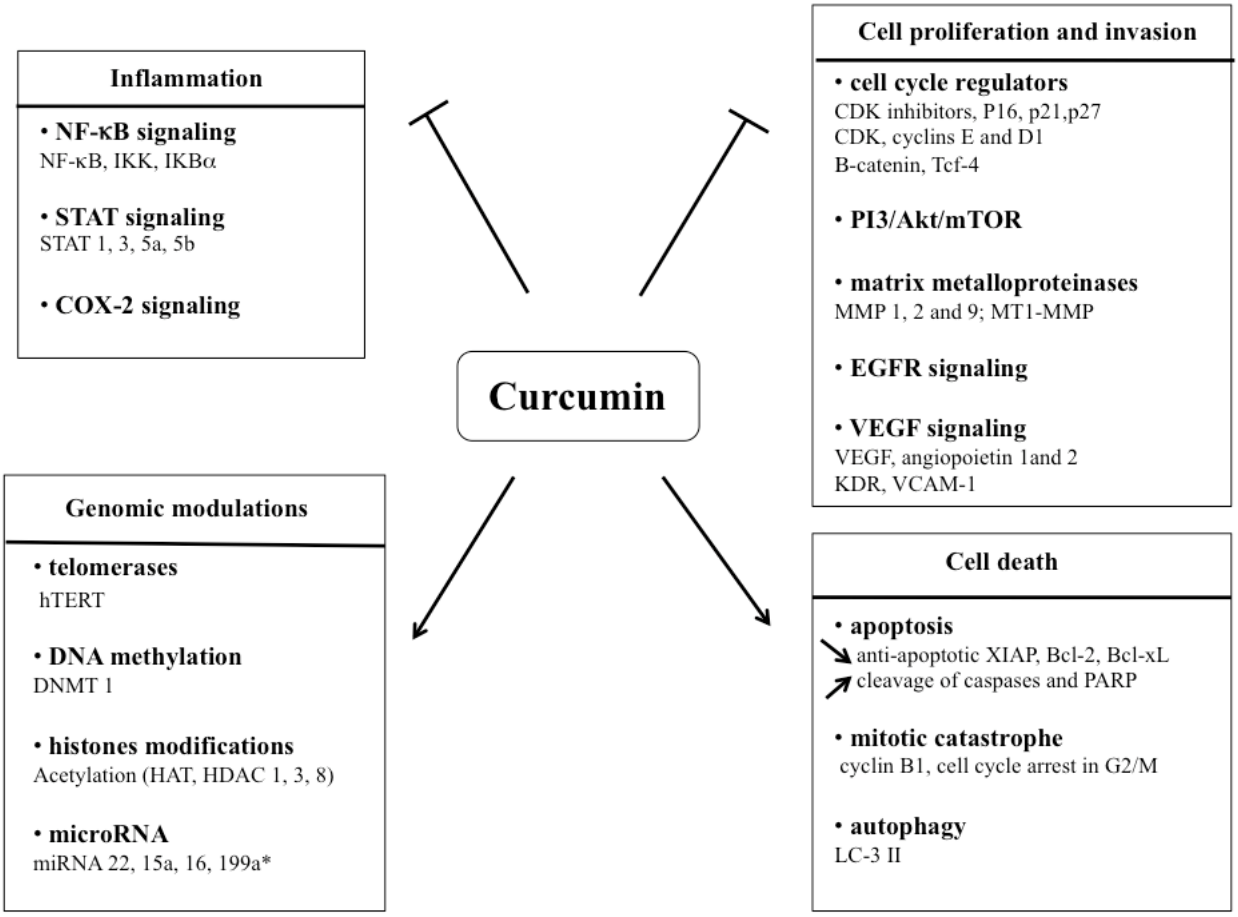

FIGURE 3: Modulation of multiple molecular targets by curcumin in cancer cells. Arrows represent induction/activation whereas blunt-ended lines represented inhibition/repression [18].

Curcumin prevents the formation of reactive oxygen species and reactive nitrogen species through activated macrophages and neutrophils via blocking NF- κB activation. This is done by preventing phosphorylation

and degradation of inhibit kappa B alpha resulting in down regulation of inducible nitric oxide synthase (iNOS) gene transcription. Reactive oxygen species causes lethal mutations. Therefore by preventing the formation of the later curcumin prevents the initiation of cancer [30, 32]. NF- κB pathway also plays a primary role in tumerogenesis. NF- κB binds to DNA and causes transcription of genes involved in tumerogenesis such as apoptotsis, inflammation and angiogenesis. I-Kappa B kinase (IKK) causes the activation of NF- κB via phosphorylation of inhibitory molecules. Curcumin blocks IKK activation and inhibits NF- κB signaling. Thus, curcumin decreases the survival and induces the apoptosis of pancreatic cancer cells [17, 18]. Although curcumin was shown to be effective against breast, pancreatic, prostate cancer, etc. it's limited bioavailability limits its therapeutic value. Numerous curcumin analogs have been made to overcome this bioavailability issue. Difluorinated curcumin (CDF) is one such analog of curcumin and the present study utilized CDF as the main drug.

1.2.3 CURCUMIN AS CHEMOSENSITIZER

Curcumin exerts chemo sensitization properties on various chemoresistant cancers by increasing the apoptosis of cancer cells along

with its cancer preventive property. Data from the earlier *in vitro* and *in vivo* studies has reported curcumin chemosensitizing properties on multiple cancers. Curcumin potentiates the affect of gemcitabine in pancreatic cancer[33]. Curcumin was shown to potentiate cytotoxic effects of doxorubicin, 5-FU and paclitaxel against prostrate cancer cells [34]. Curcumin also enhanced cytotoxicity of cisplatin against ovarian cancer cells [35]. Curcumin also proved to potentiate the activity of drugs such as gemcitabine, celecoxib, oxaliplatin, docetaxel *in vivo* [16]. Curcumin's chemosensitizing effects on multiple cancers used alone or in combination with other drugs makes it a more desirable drug for cancer therapy.

1.2.4 PHARMACOKINETICS OF CURCUMIN

The anti-cancer activity and therapeutic potential of curcumin is hampered by its poor absorption, rapid metabolism and biliary clearance. Curcumin has very low oral bioavailability. Absorbed curcumin undergoes rapid first pass metabolism and biliary clearance [17]. Phase II clinical trails on patients with advanced pancreatic cancer have showed that curcumin has potency against pancreatic cancer, but high levels of exposure were required [36].

Several drug delivery approaches have been utilized to improve

curcumin bioavailability by incorporating it into nanoparticle formulations. Oral bioavailability of curcumin has been improved by incorporating it into liposomes [37], micelles [38, 39], and nanoparticles [40-45]. The nanoparticle formulation of Poly (lactic-co-glycolic) acid encapsulated curcumin improved its oral bioavailability up to 9 fold when compared to free curcumin [46]. An *in vivo* report showed that one micelle formulation of curcumin improved its oral bioavailability upto 162 fold [39]. This improvement in oral bioavailability is due to PEG (polyethylene glycol) stabilization of nanoparticles which in turn are expected to increase the circulation time of nanoparticles. There was a report which desribed that PLGA encapsulated curcumin has higher anti-cancer activity against cisplatin resistant metastatic cancer cells when compared to free curcumin [45]. All these studies improved oral bioavailability of curcumin to a certain extent, but once curcumin is released it is susceptible for rapid metabolism and clearance. Therefore target tissue bioavailability is still a concern and requires further improvement.

1.3 DIFLUORINATED CURCUMIN (CDF)

1.3.1 ORIGIN AND MECHANISM OF ACTION

Recently some chemical derivatives of curcumin were shown to be more effective than free curcumin in eradicating chemo resistant cancer cells. A group recently studied the effect on introduction of bioisosteric fluoro substitution in curcumin and found out that because of higher metabolic stability of the C–F bond than C–H or C–OH, metabolic breakdown of curcumin slowed down and thereby the pharmacokinetic profile was improved [47, 48]. A novel synthetic analog of curcumin, 3,4-difluoro-benzo curcumin named as Difluorinated curcumin or in short CDF **(figure 4)** was developed by Fazlul H. Sarkar and his group to address the issues associated with poor bioavailability of curcumin [48].

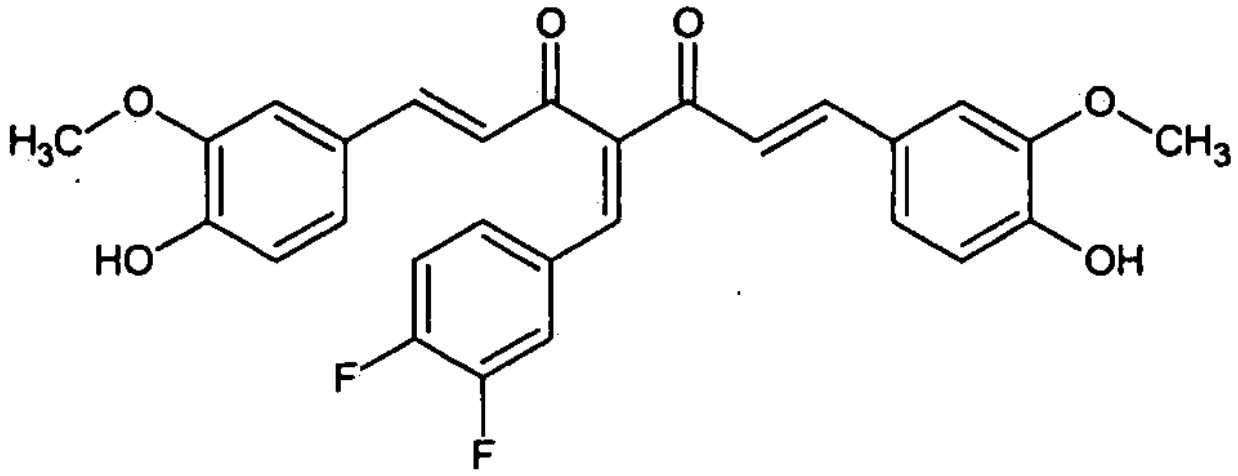

FIGURE 4: Structure of Difluorinated curcumin [31]

CDF also binds to active site of COX-2 similar to curcumin and its mechanism of action is very similar to that of curcumin [31]. Molecular docking studies showed that CDF has not induced any major steric changes when compared to the parent drug curcumin and also reduce NF-κB signaling and decrease the levels of $PGE_{2,}$ which is consistent with curcumin [49]. CDF was found to be more effective than curcumin in reducing the cell viability of pancreatic cancer cells by inducing apoptosis by reducing Akt, cyclooxygenase-2, prostaglandin E_2, vascular endothelial growth factor, and NF-κB DNA binding activity [50]. In a gemcitabine resistant pancreatic cell line, CDF upregulated miR-200 and downregulated the miR-21 (signature of tumor agressiveness) which is otherwise upregulated, causing increased expression of PTEN, a well known tumor suppressor gene [50, 51].

1.3.2 PHARMACOKINETIC ANALYSIS

CDF has 16-fold higher bioavailability when compared to curcumin with equivalent bioactivity and has higher pancreatic distribution [52]. This increased bioavailability makes it a desirable candidate for study. A recent study reported that a CDF:β-cyclodextrin complex lowered the IC50 values against multiple cancer cell lines of pancreas, breast and prostate cancer

[53]. In the present study we are focusing on making polymeric micelles incorporating CDF to improve its bioavailability.

1.4 POLYMERIC MICELLES

Polymeric micelles **(figure 5)** are amphiphilic in nature and composed of distinct hydrophilic and hydrophobic regions. When the amphiphilic polymer gets exposed to water, they phase separate forming a hydrophilic outer surface with a hydrophobic inner core forming a supramolecular core/shell structure [54, 55].

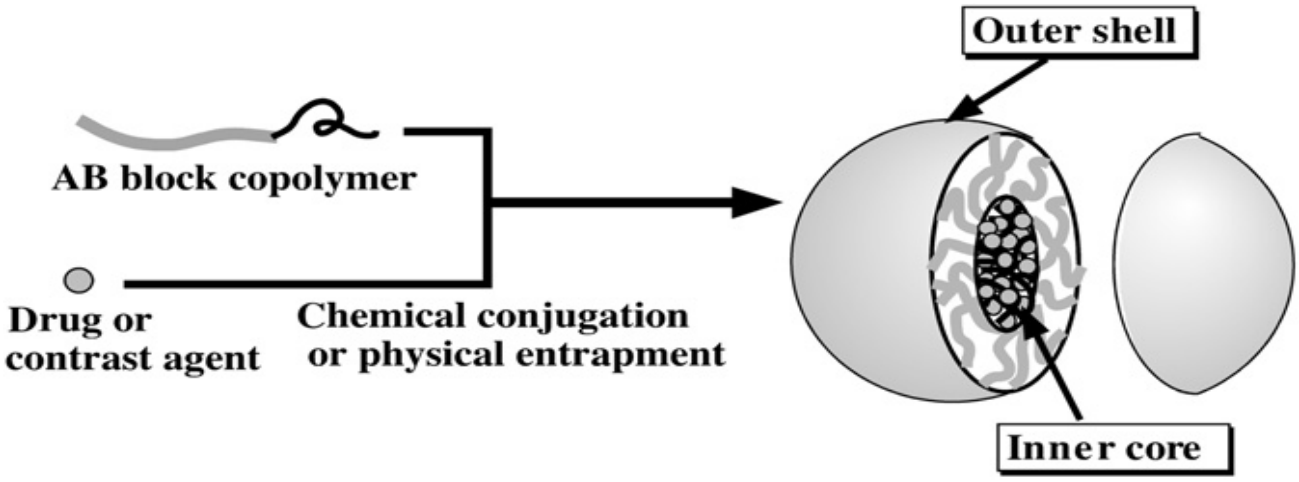

FIGURE 5: Design of a polymeric micelle carrier system[55]

These bock copolymer micelles resemble traditional low molecular weight surfactant micelles. Polymeric micelles are formed due to the self assembly of the copolymer in a solvent which is favorable for one part of

the copolymer and poor for the other. This self-assembly forms micelles.

However there are certain differences associated with this macromolecule self assembly when compared to low molecular weight surfactants. The first one being low molecular weight surfactants exist as monomer in the initial stage where there is no association, whereas for copolymers this term would cause confusion and these are called “unimers”. The hydrophobic region of these unimers are compacted into a highly coiled structure even in the nonaggregated state and these are called “unimolecular micelles” [56]. Another difference would be with the implication of use of the term “micelle”. For low molecular weight surfactants the micelle formation does not significantly vary with concentration, temperature etc., whereas the micelle formation with a copolymer is much more complex and it is a continuously changing entity. Therefore the word ‘aggregate’ or ‘micelle’ are commonly used interchangeably [56, 57].

The most important physicochemical characteristic of polymeric micelles is their high structural stability which can be attributed to the polymeric chain entanglement in the inner core of micelles. Two aspects of stability of micelles are static and dynamic [55, 58]. Static stability can be

explained as the equilibrium between a single polymer chain and a micelle's structure or by the critical micelle concentration (CMC) [59]. Generally, polymeric micelles have a low CMC value when compared to micelles formed with low molecular weight surfactants. The other aspect, dynamic stability, can be explained by the low dissociation rate of polymeric micelles. This is much more important characteristic than the static stability for *in vivo* drug delivery applications where the micelles have to undergo metabolism, excretion as well as interact with a lot of biological fluids and molecules such as lipids and proteins etc. to keep them intact in this non-equilibrium conditions. Although polymeric micelles may share the root word "micelles" they are much different than the traditional low molecular weight surfactant micelles physicochemical properties which is critical for *in vivo* drug delivery application [55, 58, 60].

1.4.1 ADVANTAGES OF MICELLES

Polymeric micelles are very small in size from 10 nm to 200 nm with a very narrow size distribution. Liver and spleen are a part of mononuclear phagocytic system (MPS) usually take up nanoparticles, depending on their surface characteristics and size. The present micelles bear PEG on their surface, which is hydrophilic and prevents them from opsonisation. This

property is advantageous for penetration into tumor cells. A phenomena that supports the tumor uptake is enhanced permeation and retention effect (EPR) leading to higher concentration at tumor site and thereby reduces toxicity [55, 61]. The small size of micelles also helps in escaping the clearance by the mono phagocytic system [62]. Since most of the drugs are of low molecular weight, incorporating them into stealth nanoparticles such as micelles can increase their bioavailability. Stealth nanoparticles have the ability to evade clearance by the body and can circulate for extended periods of time. The drug can be either chemically conjugated to the hydrophobic core part of the polymer or it can be physically entrapped by hydrophobic interaction between the hydrophobic drug and the polymer. Polymeric micelles can incorporate large number of hydrophobic drugs in their core and thereby increase the water solubility of these hydrophobic drugs. Another advantage with micelles is the ability to incorporate two or more drugs together in one formulation of micelles so these drugs can be delivered simultaneously which is an added advantage for chemotherapy especially in case of multi drug resistant tumors. Micelles can be utilized both for passive and active targeting. Passive targeting takes advantage of the size and surface properties of micelles, which is hydrophilic and causes them to circulate for a long time in the body. This longer circulation time

takes the advantage of EPR effect in tumors. Whereas for active targeting the outer surface of micelles can be modified by adding certain ligand or the substrate like some antibodies or antigens for the markers present on tumor and thus making the drug delivery specific to the tumor cells.

1.5 TESTING THE CHEMOSENSITIZING ABILITY OF CDF

In order to test the chemosensitizing ability of CDF, the model drug we chose for this study is paclitaxel. Since it is hydrophobic it can be readily encapsulated with CDF in micelles. There were several reports of taxane resistance in ovarian cancer patients [63]. So we chose ovarian cancer cell line SKOV3 which is paclitaxel resistant for testing the synergy. We tested the synergy between CDF and paclitaxel by coencapsulating CDF and paclitaxel together in one formulation along with micelles encapsulating CDF and paclitaxel individually.

1.5.1 PACLITAXEL, ORIGIN AND MECHANISM OF ACTION

Paclitaxel was isolated in 1967 from the bark of *taxus brevefolia* (northwest pacific yew tree) by Monroe E. Wall and Mansukh C. Wani and they named it taxol. It was later discovered that the endophytic fungi on the bark produced taxol. The first commercial formulation was developed by Bristol-Myers Squibb Company with the generic name as paclitaxel and

sold under the trademark Taxol ® [64, 65]. A newer formulation has been developed in which it is bound to albumin and sold under the trademark Abraxane ®.

Paclitaxel is crystalline white powder with empirical formula as $C_{47}H_{51}NO_{14}$. It is highly lipophilic and is insoluble in water. Thus, extensive research is being done on incorporating paclitaxel into different kinds of nanoparticle formulations to improve its bioavailability. Paclitaxel is approved to be used alone or with other drugs for the treatment of breast cancer, non small cell lung cancer, ovarian cancer and AIDS related Kaposi sarcoma [66].

The mechanism of action of paclitaxel involves binding to tubulin and inhibiting the disassembly of the microtubules and thereby inhibiting cell division, blocking the cell growth [67].

Nanoparticles provide advantages in chemotherapy via increasing bioavailability of drugs by slow clearance, accuracy and efficient targeting [68]. However chemoresistance has been observed in various types of cancers including breast, lung and ovarian cancer [65]. Various potential drug delivery systems have been developed for paclitaxel. Complex nanoparticles codelivering paclitaxel and twist shRNA was shown to inhibit

metastasis and increased cellular uptake in metastatic breast cancer cell lines [69]. Use of fibroblast growth factor receptor inhibitor along with paclitaxel was shown to have a synergistic effect in endometrial cancer cells [70]. A study reported that the use of combination of etoposide and paclitaxel against osteosarcoma showed a synergistic effect in the combination when compared to the drugs used alone by upregulation of Fas expression and apoptosis induction [71]. Another study demonstrated the synergy between paclitaxel and gelomulide-k, a caspase independent cell death inducing agent in a breast cancer cell line [72]. Cremophor El (CrEL) is a formuation vehicle, an integral part of paclitaxel chemotherapy. It was found to have important clinical implications associated with severe anaphtlactoid hypersensitivity reactions, hyperlipidemia and peripheral neuropathy. Alternative approaches are recommended to allow better control of toxicity of the treatment [73].

1.5.2 POSSIBLE MECHANISM OF SYNERGY BETWEEN CDF AND PACLITAXEL

In the present study we chose the cell line SKOV3, which is a paclitaxel resistant ovarian cancer cell line to test for synergy. We also tested synergy in pancreatic cancer cell line BXPC3, which is paclitaxel

sensitive.

In ovarian cancer more than 70% of the patients develop resistance to taxane therapy. Multi drug resistance (MDR) is a significant challenge occurring in cancer chemotherapy [2, 74]. Incorporating two or more different drugs in the same formulation will provide synergy and reduce the development of resistance. Although there are several mechanisms by which resistance can develop in cancer, MDR resistance is developed mainly because of upregulation of the ABC binding cassette (ABC super family of transporters), which is a frame work of membrane bound proteins that act as efflux pumps for drugs and thereby the drug concentration cannot be achieved above cytotoxic level in the cells, which reduces the efficiency of the drug. P- glycol protein (P-gp), ABCG2 and MRP-1 are the major proteins belong to ABC transporter family. P-gp is the major protein involved for MDR against taxanes, vinca alkaloids and anthracyclines [75]. A strategy to overcome MDR is to enhance systemic drug delivery by incorporating the drug into nanoparticles and also to deliver multiples drugs at the same time. Micelles are a type of nanoparticle system where incorporation of two or more drugs can be done and it also enhances the systemic circulation of the drug for long time because of the hydrophilic surface layer. The general rationale for employing combination therapy is

twofold. First, cancer cell mutations can be delayed and second, they can provide high therapeutic efficacy and higher target selectivity. Since CDF has pleiotropic effects in cancer therapy where it can act on various stages of cancer development. The main mechanism relies on its effects on transcriptional nuclear factor kappa B (NF-κB), which is master regulator in cell apoptosis, inflammation, proliferation and resistance. Curcumin was reported to down regulate three major ABC transporters including P-gp, ABCG-2 and MRP-1 [76]. So combining this pleiotropic effect of CDF along with micelle formulation and providing multi drug delivery will cause a synergistic effect in cancer therapy [77]. Paclitaxel, a cell cycle specific drug as it mainly acts on the cell division process. It prevents the formation of new cancer cells and CDF acts by increasing apoptosis of the formed cancer cells. Thus combining paclitaxel and CDF has a possibility of demonstrating synergism in cancer cell lines and potentially cancer *in vivo*.

The main objective of this study was to make a copolymer of PLGA and PEG with a disulfide bond and make micelles with that copolymer incorporating both CDF and paclitaxel to test for synergistic therapeutic effects in pancreatic (BXPC-3) and ovarian (SKOV-3) cancer cell lines.

CHAPTER 2: HYPOTHESIS AND SPECIFIC AIMS

2.1 Hypothesis: localized pancreatic cancer is a morbid form of cancer with a 5-year survival rate of only 20%. The dense desmoplastic layer surrounding the solid tumor cells is the main barrier for delivery of drugs. Curcumin Difluorinated (CDF) was found to have a more suitable pharmacokinetic profile than curcumin and it also acts as a chemo sensitizer for various chemotherapeutic drugs. In light of this idea I **hypothesize** that PLGA-S-S-PEG micelles coencapsulating CDF and paclitaxel will release the drug in presence of elevated protease levels of the tumor in a controlled manner by coordinating the release of CDF and paclitaxel resulting in a highly efficacious synergistic cancer therapy.

2.2 Specific aims

1. To fabricate polymeric micelles (PEG-SS-PLGA) coencapsulating CDF & paclitaxel

Micelles are one of the promising drug delivery systems, which can incorporate one or more hydrophobic drugs in their core thereby increasing the solubility of drugs. In the present study we will synthesize a copolymer CDF-PLGA-SS-PEG, which will be used to make micelles coencapsulating CDF and paclitaxel. This project utilizes many innovative approaches which include the use of a novel curcumin derivative, CDF, which has an improved biological stability and potency compared to curcumin. A stealth

micelle formulation that evades the MPS with tumor specificity because of the presence of a disulfide bond which breaks only at elevated protease level which is in tumor. Lastly it provides multi-therapy delivery of CDF and paclitaxel to synergistically overcome resistance.

2.Test the formulations for synergistic therapeutic efficacy in BXPC3 (pancreatic cancer) and SKOV3 (ovarian cancer) cell lines.

The proposed formulation will be utilized to coadminister CDF and paclitaxel in a controlled manner to overcome drug resistance. This novel formulation will protect CDF and paclitaxel, reduce the exposure of normal cells to paclitaxel (to reduce toxicity and increase the therapeutic-index), prolong circulation and promote tumor-specific release of PEG molecules followed by controlled degradation-dependent release of CDF and Paclitaxel in tumor. We will test the therapeutic efficacy and synergy in BXPC-3 (paclitaxel sensitive) and SKOV-3 (paclitaxel resistant) cell lines.

CHAPTER 3: MATERIALS AND METHODS

3.1 Materials

Methoxy poly (ethylene glycol) thiol (PEG-SH, Mw 5000) was bought from Jenken Technology (Beijing, China). Poly (D,L-lactide-co-glycolide) (PLGA) was purchased from Boehringer Ingelheim (502H, Ingelheim am Rhein, Germany). Cysteamine (2-Amino ethanethiol), N, N' – Dicyclohexyl carbodiimide (DCC), 2-Dimethil amino pyridine (DMAP), N-Hydroxy succinimide (NHS) and Glutathione (GSH) is obtained from ACROS organics (Morris Plains, newjersy, USA). Tetrahydrofuran (THF) was purchased from Pharmaco-AAPER (Brookfield, CT, USA). Phosphate buffered saline (PBS, pH 7.4) was bought from Fisher Bioreagents (Fair Lawn, NJ, USA). Snake skin dialysis tubing (MWCO 3,500) was bought from Fisher Scientific (Rockford, IL, USA). 3-(4,5-Dimethylthiazolyl-2)-2,5-diphenyl tetrazolium bromide (MTT) was purchased from MP Biomedicals, LLC (Solon, OH, USA). All the reagents used were of Paclitaxel was obtained from LC Laboratories (Woburn, MA, USA). Acetonitrile, acetone, methanol were purchased from Fisher Scientific (Rockford, IL, USA) and are of HPLC grade. CDF and the pancreatic cancer cell line BXPC-3 were gifted by Dr. Fazlul Sarkar, Department of Pathology, WSU / Barbara Ann Karmanos Cancer institute. The ovarian cancer cell line SKOV-3 were gifted by Dr. Olivia Merkel, Department of Pharmaceutical Sciences,

Eugene Applebaum College of Pharmacy and Health Sciences, Wayne State University.

Both cancer cell lines BXPC-3 and SKOV-3 were maintained in RPMI- 1640 (ATCC, Manassas, VA, USA) supplemented with 10% fetal bovine serum (FBS), 100 units/ml Penicillin and 100 µg/ml Streptomycin. Cells were cultured in a 5% CO_2-humidified atmosphere at 37 °.

3.2 METHODS

3.2.1 Fabrication of micelles encapsulating CDF, Paclitaxel and coencapsulating both CDF & paclitaxel

3.2.1.1 Synthesis of PEG-SS-PLGA-CDF

Briefly, 1 g (0.1 mmol) of PEG-SH (Mw 5000) and 0.77 g (10 mmol) of cysteamine were dissolved in methanol and allowed to react at room temperature by continuous stirring for 24 hours to form PEG-SS-NH_2 **(figure 7)**. Then the reaction mixture was dialyzed against methanol for two days and collected upon freezing and lyophilization for 48 hours to remove excess solvent.

For the preparation of the CDF-PLGA conjugate **(figure 6),** equimolar ratios of CDF (33.43 mg, 0.1 mmol) and PLGA-COOH (679 mg, 0.1mmol) were dissolved in 10 ml of THF in presence of 0.2 mmol DCC and 0.2 mmol DMAP at room temperature by continuous stirring for 24 hours. Then

the CDF-PLGA conjugate was precipitated out with petroleum ether and centrifuged at a speed of 10000 rpm to collect the precipitate. To purify the formed conjugate, the precipitate was dissolved in methylene chloride and again precipitated out with petroleum ether. This purification step was repeated out 3 times. Final sample was lyophilized after dissolving in 5 ml of methylene chloride.

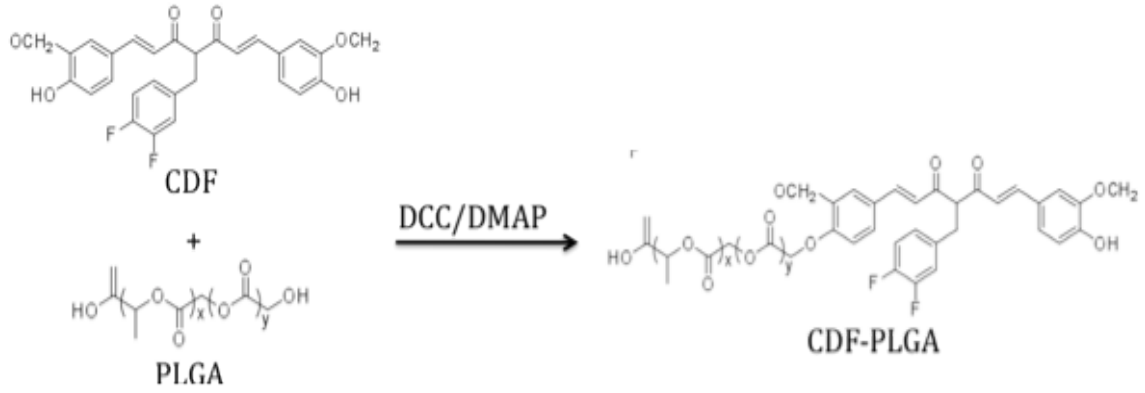

FIGURE 6: CDF-PLGA conjugate formation

To synthesize CDF-PLGA-SS-PEG **(figure 7)**, 0.05 mmol PEG-SS-NH_2 and 0.05 mmol PLGA-CDF were dissolved in 10 ml of methylene chloride in presence of DCC & NHS and reacted for 24 hours with continuous stirring. Then the formed conjugate was precipitated out with petroleum ether and centrifuged at a speed of 10000 rpm to collect the precipitate. To purify the formed conjugate, the precipitate was dissolved in methylene chloride and again precipitated out with petroleum ether. This

purification step was repeated out 3 times. The final sample was lyophilized after dissolving in 5 ml of methylene chloride.

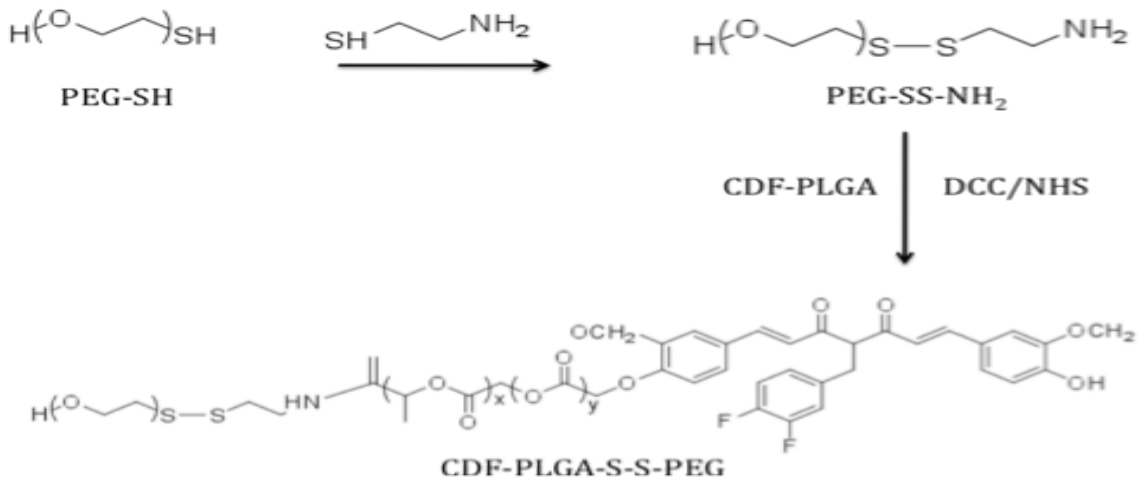

FIGURE 7: PEG-SS-NH_2 and CDF-PLGA-SS-PEG formation

3.2.1.2 Characterization of conjugates

The Fourier - transformation infrared absorption (FTIR) spectra were recorded for the synthesized conjugates using an FTIR spectrometer (Jasco FTIR-4200, Tokyo, Japan) and a sample holder (Jasco ATR PRO450-S) at 400-4,000 cm^{-1} at room temperature. The dried samples were analyzed directly with the FTIR spectrometer. The nuclear magnetic resonance (^{1}H-NMR) spectrum was recorded on a Varian spectrometer operating at 400 MHZ using $CDCl_3$ (Deuterated chloroform) as the solvent. Thin layer chromatography (TLC) was performed for the CDF-PLGA conjugate using ethyl acetate : n-hexane in the ratio of 1:1 was used a

mobile phase. Acetone was used as stationary phase. Two drops were made separately on a TLC plate containing CDF and the CDF-PLGA conjugate dissolved in acetone. The results were observed under uv light.

3.2.1.3 Preparation of CDF-PLGA-S-S-PEG micelles encapsulating CDF and/or Paclitaxel

All Micelle formulations were prepared by phase inversion using dialysis. A solution of 100 µg/ml of CDF-PLGA-S-S-PEG was prepared in THF. To make CDF loaded micelles 10 wt% CDF (0.3 mg) was added to the conjugate solution. Similarly, to make paclitaxel-loaded micelles 10 wt% of (0.3 mg) paclitaxel was added to the conjugate solution in THF. For both CDF and paclitaxel loaded micelles, 10 wt% of CDF (0.3 mg) and paclitaxel (0.3 mg) were added to the conjugate solution. Micelles were prepared by adding 100 µg/ml of the conjugate solution into 1 ml of deionized water which was under stirring at 1200 rpm. Then the emulsion was transferred into a dialysis bag and dialyzed against water for 24 hours by replacing with fresh water at 2 hour intervals to remove the organic solvent and form micelles. Since both CDF and paclitaxel are hydrophobic they will readily be encapsulated within the hydrophobic core of micelles. The micelles were collected after lyophilization.

3.2.2 Morphological and physicochemical characterization of micelles

3.2.2.1 Percentage Drug loading and percentage encapsulation efficiency for micelles

To determine the CDF content in micelles, 5 mg micelles were taken and dissolved in 5ml acetone and filtered and analyzed for CDF content on a Varian CARY 50 Bio / UV-VIS spectrophotometer at 355 nm. A standard curve of CDF in acetone was made and used for calculating drug content (table 1).

To determine the paclitaxel content in micelles, 5 mg of micelles were taken and dissolved in 5ml of acetonitrile and was filtered and analyzed for paclitaxel content by HPLC. The mobile phase consisted of water/acetonitrile in the ratio of 40:60 v/v. An ODS hypersil column with 250 × 4.6 (mm) in dimensions was used. The column temperature was maintained at 25 °C. The flow rate was set at 1.0 ml/min and the detection wavelength was 228 nm. The sample solution was injected at a volume of 10 µL. The standard curve for paclitaxel was made with the same HPLC method using acetonitrile as solvent and was used for calculating drug content (table 2).

$$\text{Percentage drug loading content} = \frac{\text{Weight of drug in micelles}}{\text{Total weight of micelles}} \times 100$$

$$\text{Percentage entrapment efficiency} = \frac{\text{Weight of drug in micelles}}{\text{Weight of initial drug taken}} \times 100$$

3.2.2.2 Micelle size and zeta potential

The particle size of micelles was determined by reconstituting micelles in DI water to make 0.1% w/v dispersion. This was subjected to size analysis by using a 90Plus Particle Size Analyzer (Brookhaven Instrument Corporation). Mean values were calculated. 5 runs for each formulation were recorded.

The morphology and size of micelles were studied using an atomic force microscope (AFM) Nanoscope III (Digital instruments/Veeco, Plainview, Santa Barbara, CA, USA) with an E scanner probe in the tapping mode. A drop of micelle suspension in DI water was put onto a coverslip and dried in a dessicator and observed by AFM.

The zeta potentials of micelles were determined by making a 0.1% w/v dispersion in deionized water and subjected to zeta potential analysis on a 90plus particle size analyzer (Brookhaven instrument corporation). Mean values were calculated. 10 runs for each formulation were recorded.

3.2.2.3 Critical micelle concentration (CMC) determination

PLGA-S-S-PEG polymer can self assemble to form micelles due to the presence of the hydrophobic PLGA block, which aggregates in water to

form the core of the micellar structure with hydrophilic PEG as the outer layer. This micelle formation is commonly monitored by changes in the fluorescence spectrum of a pyrene probe, which preferably partitions in the micelle core. The encapsulation causes changes in the photophysical properties of the nanoparticle under investigation. With this method we monitor the changes in the ratio of pyrene emission spectra intensities at λ = 372 nm and at λ = 384 nm due to the migration of pyrene into the more hydrophobic region of newly formed micelles from the aqueous media [78, 79]. The concentration of pyrene in the aqueous media was 0.2 μg/ml. The concentration of copolymer varied from 1 to 200 μg/ml. The micelles are formed in presence of the same concentration of pyrene with varying concentrations of polymer. These solutions were kept at room temperature under continuous stirring to allow the organic solvent to evaporate while forming micelles. Then fluorescence spectra were recorded with an excitation wavelength of 334 nm and emission fluorescence at 372 nm and 384 nm using a Fluoromax-3 Spectro Fluorometer (Horiba scientific). By plotting I_{372}/I_{384} versus the logarithm of the concentration of CDF-PLGA-S-S-PEG, sigmoidal curves were obtained where a sharp increase of the fluorescence intensity ratio (I_{372}/I_{384}) was observed with increase in copolymer concentration.

3.2.3 Invitro drug release studies

The drug release profiles of CDF and paclitaxel loaded micelles were studied by a dialysis method. Lyophilized micelles of 5 mg containing encapsulated CDF and paclitaxel are suspended in 5 ml of 0.5% tween 80 PBS at pH 7.4 and transferred to a dialysis tube. Then the tubes were immersed in 25 ml of release media (PBS without GSH, 20 μM GSH, 5 mM GSH, 20 mM GSH) 0.5% tween and also in PBS without GSH as a control and were gently shaken. At predetermined intervals one ml of two samples were collected from each group and lyophilized. The release medium was replaced with the same amount of new media. One sample was used for CDF analysis by UV-VIS spectrophotometer and the other one was used for paclitaxel analysis by HPLC (waters 2695 with waters 2996 photodiode array detector). The *in vitro* release profile of the free drug was also studied in 0.5% tween containing PBS.

3.2.4 Cell culture studies

3.2.4.1 Invitro cytotoxicity studies

These studies were done in both the BXPC-3 (pancreatic cancer) cell line and the SKOV-3 (human ovarian carcinoma) cell line. *In vitro* cytotoxicity of all the formulations of CDF micelles, paclitaxel micelles and micelles encapsulating both CDF and paclitaxel were evaluated in both cell

lines. Both cell lines were cultured in RPMI-1640 medium containing 10% fetal bovine serum and 1% penicillin-streptomycin.

In vitro cytotoxicity was evaluated by 3- (4,5-dimethylthiazol-2-yl)-2,5-dipheny-ltetrazolium bromide (MTT) assays for both cell lines. The same procedures were followed for both cell lines. The cells were seeded into 96-well plates at a density of 5000 cells per well and incubated at 37 °C in humidified atmosphere with 5% CO_2 for 24 hours. Then the media was removed and cells were treated with media containing various drug concentrations of CDF and/or paclitaxel. BXPC-3 cells were tested for paclitaxel in the concentration range of 1000 nM to 0.001 nM for free drug as well as micelle formulations and for CDF in the concentration range of 5 μM to 0.0002 μM for free drug and micelle formulations. Similarly SKOV-3 cells were tested for paclitaxel in the range of 5 μM to 0.001 μM and CDF in the range of 50 μM to 0.2 μM for free drug and micelle formulations. The same procedure was followed for both cell lines using control micelles without any drug. The cytotoxicity was checked at three time points after drug exposure at 24 h, 48 h and 72 h. After specified durations, 22 μL of 5 $mgmL^{-1}$ of MTT prepared in PBS was added to each well. The plate was incubated for 2 h at 37 °C allowing viable cells to metabolically reduce yellow colored MTT into the purple colored formazan compound. At the end

of the 2 h period the medium was removed from the wells and 100 µL of dimethylsulfoxide (DMSO) was added to dissolve the formazan crystals and the plate was shaken for 20 min. The optical density (OD) was measured 595 nm with a Synergy H_1 hybrid reader (Biotek). Cell viability (%) was calculated as (OD of test group/OD of control group) × 100.

3.2.4.2 Evaluation of combination effect of CDF and paclitaxel

The statistical analysis of the drug combination effect was done by the Chou-Talalay method [80]. This method is based on the median-effect equation that describes the dose-effect relationship in a most simple way as shown below

$$\frac{fa}{fu} = \left(\frac{D}{Dm}\right)^m$$

Where D is the dose (or concentration) of a drug, f_a is the fraction affected by D and f_u is the fraction unaffected (i.e., $f_u = 1 - f_a$). D_m is the median-effect dose (IC_{50} incase of cell killing) that inhibits the system under study by 50%, and *m* is the coefficient signifying the shape of the dose-effect relationship, where *m* = 1, > 1, and < 1 indicate hyperbolic, sigmoidal, and flat sigmoidal dose-effect curves, respectively [80, 81].

The median effect equation can be extended to multiple drugs with mutually exclusive drug effects, for example a combination of two drugs (D_1

and D_2), the equation can be defined as below:

$$\left[\frac{(f_a)_{1,2}}{(f_u)_{1,2}}\right]^{1/m} = \left[\frac{(f_a)_1}{(f_u)_1}\right]^{1/m} + \left[\frac{(f_a)_2}{(f_u)_2}\right]^{1/m} = \frac{(D)_1}{(D_m)_1} + \frac{(D)_2}{(D_m)_2}$$

where $(fa)_{1,2}$ is the fraction of the population effect in combination of two drugs, $(f_a)_1$ and $(f_a)_2$ are fractions of affected cell population in presence of single drug D_1 and D_2, respectively. Based on the above equations Chou and Talalay in 1983 introduced the termed combination index (CI) for the evaluation of synergism or antagonism between two drugs as:

$$CI = \frac{(D)_1}{(D_x)_1} + \frac{(D)_2}{(D_x)_2}$$

Where $(D_x)_1$ and $(D_x)_2$ are the doses of drug D_1 and D_2 to achieve a certain effect x, respectively. $(D)_1$ & $(D)_2$ are the doses of the drugs D_1 and D_2 in combination to achieve the same effect. CI < 1, = 1 and > 1 indicates synergism, additive effect and antagonism, respectively. The CI value can be categorized as follows: CI < 0.1 very strong synergism; 0.1-0.3 strong synergism; 0.3-0.7 synergism; 0.7-0.9 moderate/slight synergism; 0.9-1.1 additive; 1.1-1.45 slight/moderate antagonism; 1.45-3.3 antagonism; 3.3-10 strong antagonism; CI >10 very strong antagonism [81]. The dose reduction index is another important parameter that can be obtained from the median effect/CI model, which is defined as:

$$(DRI)_1 = \frac{(D_x)_1}{(D)_1}$$

The DRI value indicates how much of each drug in combination can be reduced, compared to the doses of each drug alone. CI and DRI values allow the quantitative determination of a synergistic effect between two drugs. This model will be used for our study of synergism between CDF and paclitaxel.

CDF concentration (µg/ml)	Absorbance
1	0.0946
2	0.189
3	0.284
4	0.379
5	0.474
8	0.759
10	0.949
15	1.354
20	1.775
25	2.759

Table 1: Standard graph of CDF in acetone by U.V spectrophotometry at wavelength 355 nm. ($y = 0.117x – 0.3386$ and $R^2 = 0.9454$)

Paclitaxel concentration ((µg/ml)	Area of elution peak
0.5	26725
1	47211
5	234311
10	213826
20	437213
50	1063001
100	1932855
200	3898352
500	9610858
1000	19116591

Table 2: Standard graph of paclitaxel in acetonitrile by HPLC at wavelength 225 nm. ($y = 19067.1742x + 61071.8897$ and $R^2 = 1$)

CHAPTER 4: RESULTS AND DISCUSSION

4.1 Characterization of conjugates

The schematic approach for the synthesis of CDF-PLGA-S-S-PEG was shown in figure 6 and 7. The synthetic procedure included 3 steps: (1) the preparation of the CDF-PLGA conjugate, which was prepared by the esterification between carboxyl-terminated PLGA and CDF in presence of DCC and DMAP (figure 6). (2) The disulfide PEG was synthesized by the reaction of PEG-thiol and cysteamine in methanol forming PEG-SS-NH_2. An excess of unreacted cysteamine was removed by dialysis. (3) CDF-PLGA-SS-PEG was prepared by the coupling reaction between the amino and carboxyl group of activated PLGA and PEG-SS-NH_2 respectively (Figure 7).

The structures of the formed conjugates were verified with ^{1}H NMR and FTIR. In the ^{1}H NMR spectrum of the copolymer (figure not shown), four major peaks correspond to PLA (poly lactide), PGA (poly glycolide) and PEG segments appeared at 1.5 ppm (methyl of PLA) and 5.16 ppm (methine of PLA) and at 3.5 and 3.7 ppm (methylene of PEG) and at 4.8 ppm (methylene of PGA) [78, 82]. CDF peaks were observed at 6.4, 6.7, 7.1, 7.4 and 7.6 ppm.

FTIR spectra were also used to confirm the formation of conjugates. As shown in figure 8, the typical C=O band at 1747 cm^{-1} in CDF-PLGA-S-S-PEG conjugate was appeared due to the presence of PLGA. The bands at 2865 cm^{-1} and 2857 cm^{-1} are ascribed to the asymmetric and symmetric CH_2 stretching band of the PEG chains present in the CDF-PLGA-S-S-PEG conjugate. With TLC, a distinct spot for CDF and a band for CDF-PLGA conjugate was observed which indicate the formation of the conjugate.

The presence of these characteristic peaks relevant to CDF, PEG and PLGA supports the successful synthesis of the copolymer. Since this formed copolymer is amphiphilic as it has hydrophilic PEG attached to hydrophobic PLGA. Thus it will be able to form micelles with an outer PEG layer and inner PLGA core. Here PEG is attached to PLGA via a disulfide bond which we anticipate to be cleaved in elevated protease levels in tumor cells followed by hydrolysis of PLGA will release the drug from the micelles.

4.2 Physicochemical characterization of micelles

4.2.1 Drug loading and encapsulation efficiency for micelles

Formulation	Wt% Drug loading	% Encapsulation efficiency	Size (nm)	Zeta potential (mV)
CDF-PLGA-SS-PEG micelles	0.4	8%	145 ±11	1.07±2.05
PLGA-SS-PEG micelles encapsulating CDF	8.9	89%	165±18.2	-0.43±3.21
PLGA-SS-PEG micelles encapsulating Paclitaxel	9.5	95%	171±17.4	0.89±1.45
PLGA-SS-PEG micelles coencapsulating CDF & Paclitaxel	CDF-8.7% Paclitaxel-9.1%	CDF-87% Paclitaxel-91%	208.5±21.3	1.12±2.38

Table 3: Drug loading, encapsulation efficiency, size and zeta potential measurements of micelle formulations

4.2.2 Micelle size and zeta potential

The size and zeta potential measurements are given in **table 1** for all the micelle formulations. The zeta potential of all micelle formulations were about neutral. This helps in preventing the non-specific adsorption of proteins on to the surface of micelles and prevents the clearance from the monophagocytic system, which hinders the drug from reaching its targeting site [83]. The morphology of micelles was studied by AFM. The micelles were made initially with 1mg/ml of conjugate concentration and observed

micelle size was more than 300 nm (FIG 9). Then we reduced the concentration of the conjugate to make micelles with 100 µg/ml. The AFM images were taken and the size of micelles was well below 60 nm (FIG 10). The micelles were spherical. The micelle size was further confirmed by DLS measurements showed in Table 3. The micelle size is larger with DLS measurement which might be due to the presence of aggregates. The dehydration of micelles and the shrinkage of the PEG shell induced by water evaporation under high vacuum conditions before AFM observation led to smaller size measured by AFM. This smaller size prevents the uptake of micelles by the MPS and helps in penetrating the tumor by EPR effect.

4.2.3 Critical micelle concentration (CMC)

Micelles were prepared by the dialysis method with the CDF-PLGA-SS-PEG conjugate with increasing concentrations from 1 to 300 µg/ml. At a certain concentration the micelles are formed. That concentration is defined as critical micelle concentration (CMC).

The CMC value was determined using pyrene as a probe. The plot of fluorescence intensity ratio versus log concentration is shown in figure 10. As indicated from the graph, the ratio of intensities is relatively constant until a certain point where there was an abrupt increase in this ratio. This

indicates the formation of micelles leading to the migration of pyrene into more hydrophobic PLGA core of the micelles. The CMC value was found to be 100 µg/ml. This low CMC value is an important feature in terms of drug delivery applications of micelles by providing them thermodynamic stability for *in vivo* use in a very dilute environment.

4.2.4 *In vitro* drug release studies of micelles

In vitro drug release studies were carried out on CDF-PLGA-S-S-PEG micelles coencapsulating both CDF and paclitaxel in presence and absence of GSH at various concentrations to get a release profile estimate of micelles within a reductive environment. The release of the drugs were studied at 20 µM GSH which is the concentration of GSH in plasma, 5 mM GSH which resembles the concentration of GSH in the cytosol and subcellular compartments and at 20 mM which is the concentration of GSH in tumor microenvironment [84, 85]. The release was also studied in presence of PBS (pH=7.4, 0.5% tween 80) without GSH. The release study with free CDF and paclitaxel was also done as a control in PBS. The results are shown in Figure 11. The release of CDF and paclitaxel from micelles was very slow in PBS without GSH. Only 4.6% CDF and 3% paclitaxel were released in the first 4 h in just PBS without any GSH. Whereas 4.8%, 4.9% and 24% of CDF and 4.9%, 10.26% and 21.7%

paclitaxel were released in 20 μM, 5mM and 20 mM GSH respectively. So at highest GSH concentration i.e. at 20 mM GSH the drug release was fastest because of the increased cleavage of disulfide bond thereby shedding the PEG coating followed by hydrolysis of PLGA which further releases the encapsulated drug by diffusion.

Within 24 h 55% of CDF and 52.6% paclitaxel were released in 20 mM GSH which is much higher when compared to the release in presence of 20 μM and 5mM GSH. This indicates that the drug is released from micelles fast only when it is exposed to a highly reductive environment. In plasma and cytosol, where the GSH concentration is low, the drug release is much slower. This indicates that the micelles will not release any drug in those areas as the disulfide bond cannot be cleaved at these low GSH levels. The release of drugs from micelles without redox sensitivity was even slower in the absence of GSH or at 20 μM GSH. Around 80% of the drug was released in 72 h at 20 mM GSH concentration.

Based on our results we have shown that a certain degree of disulfide bond breakage was necessary to release CDF and paclitaxel from the inner core of micelles, which is higher in tumor cells because of high GSH concentrations. These micelles are likely to be stable in plasma on exposure to low GSH concentration (20 μM) and even at cytosolic GSH

concentration (5 mM) the drug release was slow indicating the micelles would remain intact when intravenously administered, and rapidly release the drug in the tumor microenvironment. Therefore, PLGA-SS-PEG micelles coencapsulating CDF and paclitaxel can be a highly promising drug delivery system to achieve intracellular fast release of anticancer drugs and enhance their therapeutic efficacy.

4.2.5 Cell culture studies

4.2.5.1 Invitro cytotoxicity studies

The cytotoxicity effect of free CDF, free Paclitaxel, CDF micelles, paclitaxel micelles and micelles coencapsulating CDF & paclitaxel were evaluated on BXPC-3 (pancreatic cancer) and SKOV-3 (ovarian cancer) cells at the end of 24, 48 and 72 hours of incubation. The IC50 values for each formulation on BXPC-3 cells and SKOV-3 cells are represented in table 4 and table 5 respectively.

The results of the cytotoxicity experiment on BXPC-3 cells with CDF micelles, paclitaxel micelles, micelles coencapsulating both CDF and paclitaxel micelles and control micelles were shown in **figure 12, 13, 14 and 15** respectively. The results of the cytotoxicity experiment on SKOV-3 cells with CDF micelles, paclitaxel micelles, micelles coencapsulating both CDF and paclitaxel micelles and control micelles were shown in **figure 16,**

17, 18 and 19 respectively. The control micelles used were CDF-PLGA-SS-PEG micelles without any encapsulated drug as these micelles had only 0.4% CDF loading. This didnot have any antiproliferative effect at the dilutions of different concentrations of CDF and Paclitaxel used for the MTT assay. So it was used as control and the same conjugate was used to prepare micelles encapsulating CDF, paclitaxel and both CDF and paclitaxel. The control micelles were tested at the same dilutions as CDF micelles.

A time and concentration dependent antiproliferative effect was displayed with all the formulations in both cell lines. As the concentration of the drug and exposure time increases, the anti proliferative effect is increased. At the 72 h time point, in both cell lines, maximum cell death was observed and it was much higher with the micelles coencapsulating CDF and paclitaxel. The IC50 values were less with micelles than free drug for both cell lines at the 72h time point.

Figure 12 and **15** represents the % cell viability of BXPC-3 cells and SKOV-3 cells upon incubation with several concentrations of free CDF and CDF micelles at 24 h, 48 h and 72 h time points. At the 24 h time point for BXPC-3 cells, free CDF was more effective than micelles. At 48 and 72 h time points CDF micelles are as effective as free drug. There is a

concentration dependent antiproliferative effect displayed both by free CDF and CDF micelles in both cell lines. The IC50 values were significantly lowered at 72 h time point in BXPC-3 and SKOV-3 cells indicating a time dependent antiproliferative effect of free CDF and CDF loaded micelles. The IC50 value was 2.4 μM for free CDF and 2.1 μM for CDF loaded micelles in BXPC3 cells and 16.37 μM for free CDF and 14.7 μM for CDF loaded micelles which indicated micelles are as efficient as free drug. Formulating CDF into micelles did not hamper its anti proliferative effect. We anticipate that these micelles are advantageous when we administer the drug *in vivo* in which case these micelles can remain intact until exposed to a highly reductive environment suchas tumor cells (20 mM GSH) as it was shown in the drug release studies and cytotoxic effect of free drug on normal cells can be reduced.

Figure 13 and **16** represents the % cell viability of BXPC3 and SKOV3 cell respectively upon incubation with several concentrations of free paclitaxel and paclitaxel loaded micelles at 24 h, 48 h and 72 h time points. From **figure 13**, for BXPC3 cells the IC50 value for paclitaxel was 527 nM at 24 h, 45.82 nM at 48 h and 10.4 nM at 72 h time points. The reason for this significant difference might be due to the mechanism of action of paclitaxel, which is a mitotic inhibitor and cell cycle specific. So

until the 24 h time point the cells are not in active proliferative stage and so the effect of paclitaxel was not significant at this time when compared to 48 h and 72 h where paclitaxel actually started showing its anti proliferative effects on BXPC-3 cells. At all time points paclitaxel loaded micelles are as effective as free paclitaxel. At the 48 h time point micelles have shown more anti proliferative effect when compared to free drug at all concentrations for BXPC-3 cells. From figure 16, for SKOV-3 cells which are resistant to paclitaxel there was very less difference in IC50 values at various time points. The IC 50 was 11.32 μM for free paclitaxel at 24 h and 8.22 μM at 72 h time point. At all time points the IC50 values for paclitaxel loaded micelles were lower than free drug. In SKOV-3 cells a high amount of paclitaxel is required to produce cytotoxicity.

Figure 14 and **17** represent the % cell viability of BXPC-3 and SKOV-3 cells respectively when a combination of CDF and paclitaxel was used as free drugs and also coencapsulated in micelles and tested at the end of 24 h, 48 h and 72 h. BXPC-3 is sensitive cell line to both CDF and paclitaxel. From **figure 14**, on BXPC-3 cells the antiproliferative effect is significantly increased for the drug combination for free drugs as well as in micelles at all time points and all the concentrations tested. Except for the 24 h time point from **table 1**, IC50 values were less for the micelle

formulation than for the free drug. At 24 h the release of drug from micelles might be less so less drug is available when compared to free drug. The IC50 values significantly decreased in combination from 2.4 μM to 0.1 μM of CDF and 10.4 nM to 7.5 nM paclitaxel at 72 h. From **figure 17**, on SKOV-3 cells the combination of CDF and paclitaxel has shown very significant anti proliferative effect when compared to that of CDF and paclitaxel alone. The micelles encapsulating both CDF and paclitaxel have shown very similar antiproliferative effect when compared to the combination of both free drugs except at 24 h. SKOV-3 cells are much more sensitive to the combination when compared to individual drugs. From **table 2** the IC50 value is 16.37 μM for CDF and 8.22 μM for paclitaxel whereas in combination it was 9.8 μM for CDF and 1.56 μM for paclitaxel at 72 h.

Based on cell viability study results we assume that PLGA-SS-PEG micelles incorporating CDF, paclitaxel and both of those are as effective as free drugs during MTT assay. We believe based on these results as well as from the drug release study results that CDF and paclitaxel when incorporated into micelles will work more efficiently than the free drug form *in vivo*. The hydrophilic PEG layer of micelles make them circulate for longer period in the body and thus it provides more chance to release the

drug in tumor when exposed to high glutathione levels of tumor cells (20 mM). Even though there is glutathione present in the cytoplasm its concentration is much lower (5mM) when compared to tumor cells so the degradation of micelles is less likely in those regions. Similar is the case with plasma where the GSH concentration is 20 μM to which the disulfide bond in micelles is not susceptible. Because of the enhanced permeation and retention effect in tumor cells and size of our micelles which is less than 200 nm, and PEG coating it is more likely that micelles will penetrate tumor cells more effciently and then by reduction of the disulfide bond within the tumor cells they will release the drug internally. Therefore the overall cytotoxicity to the normal cells can be reduced with this formulation.

4.2.5.2 Evaluation of combination effect of CDF and paclitaxel in micelles

In order to test the chemo sensitizing ability of CDF we chose paclitaxel as the model drug. We tested the synergistic effect of CDF and paclitaxel against BXPC-3 and SKOV-3 cells. The combination index values are given in **table 6 and 7** for SKOV-3 and BXPC-3 cells respectively.

The SKOV-3 cell line used is a model for paclitaxel resistance as

very high concentration of drug is required to obtain get 50 % cell killing (IC50 8.2 μM). Acoordingly we used micelles coencapsulating CDF and paclitaxel and CDF micelles and paclitaxel micelles to test the synergy. From the combination index values given in **table 6** for SKOV-3 cells**,** the free drug combination at 24 h has a combination index (CI) value equal to 1, indicating the additive effect at that point. The degree of synergy increased as the exposure time of the drug to the SKOV-3 cells increased showing maximum synergy at the 72 h time point. The synergy between CDF and paclitaxel further increased by coencapsulating both drugs in the micelle formulation in which CI was 0.62. the CI for free drug combination was 0.66. By coencapsulating the two drugs in one micelle formulation, when used *in vivo* it is possible for both the drugs to reach and penetrate the tumor cell at the same time and release the drug inside the tumor to complement each other inside the cell to produce a maximum synergistic effect. When used in combination in micelles, the IC50 values for both CDF and paclitaxel were reduced from 14.7 μM and 7.9 μM to 8.2 μM and 1.48 μM respectively. P-gp is the major protein involved for MDR against taxanes. This is a membrane bound protein and acts as efflux pump for drugs and so the drugs cannot achieve the required concentration to produce a cytotoxic effect. Curcumin was found to down regulate these

ABC transporters and thereby it can increase the sensitivity of cells otherwise resistant paclitaxel.

Similarly from **table 7,** combination effect values against BXPC-3 cells also indicate synergy between CDF and SKOV-3 cells. Since CDF has multiple effects such as inhibiting NF- KB, EGFR, HER2, STAT-3 and also inhibits ABC transporters. Because of this ability of CDF to effect different molecular mechanisms of cancer it causes apoptosis of cancer cells, whereas paclitaxel being a mitotic inhibitor acts on cell cycle and inhibits the formation of new cells. So when they are used in combination, synergy is produced by effecting cancer cell growth during cell division and by causing apoptosis at the same time thereby increasing the effectiveness of therapy.

Dose reduction index values (DRI) are calculated and given in **table 8** for SKOV-3 and BXPC-3 cells to estimate the reduction of the overall dose when coencapsulated together in micelles compared to CDF micelles and paclitaxel micelles to produce 50 % cell killing at the 72 h time point where maximum synergy was observed. In case of SKOV-3 cells there was a 5.3 fold reduction in paclitaxel and a 1.8 fold reduction in CDF concentration was observed. For BXPC-3 cells, a 16 fold reduction in CDF

and a 1.5 fold reduction in paclitaxel was observed. In SKOV-3 cells which requires a high concentration of paclitaxel, micelles coencapsulating CDF and paclitaxel will be advantageous to reduce the overall dose of paclitaxel when combined with CDF to reduce the overall toxicity associated with using high amounts of paclitaxel. Based on these results we concluded that the combination of CDF and paclitaxel in micelles formulation will help to reduce the dose of the individual drugs in combination therapy and thereby less drug is sufficient to produce cytotoxic effect to cancer cells. Combining different drugs in one formulation is advantageous mainly in MDR cancers. The drug combination will also helps in reducing the lethal side effects caused by cancer chemo therapeutics as the overall dose can be reduced.

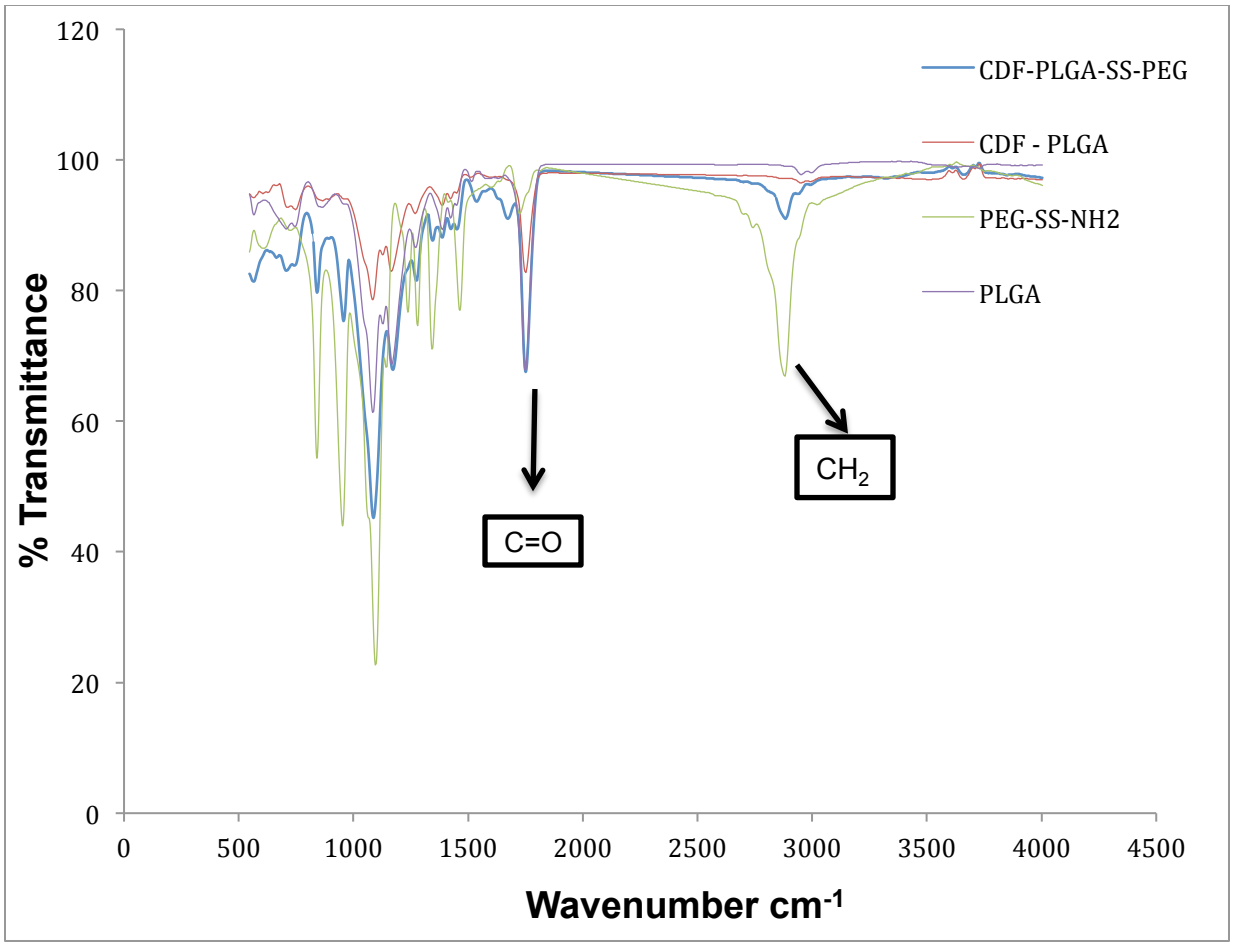

FIGURE 8: FTIR spectra of synthesized conjugates

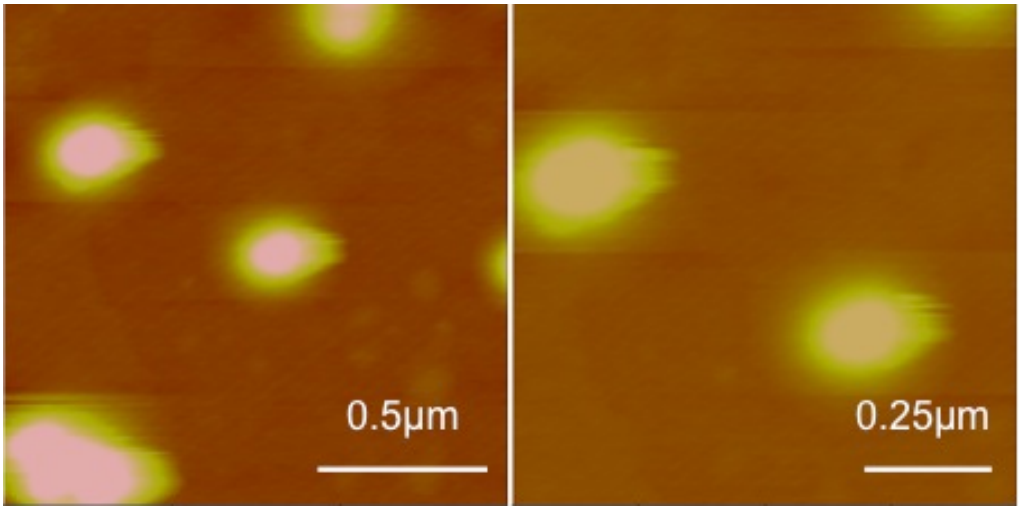

Figure 9: AFM images of CDF-PLGA-SS-PEG micelles with conjugate concentration of 1 mg/ml.

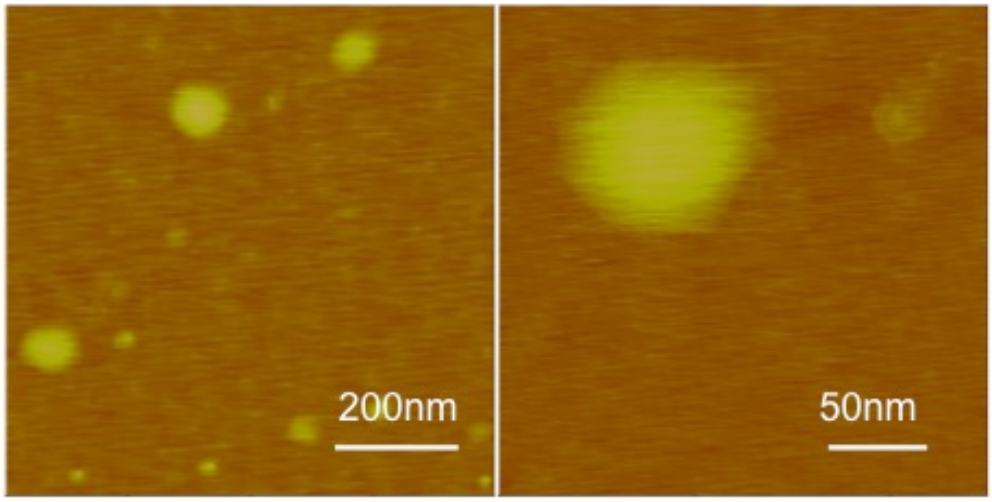

Figure 10: AFM images of CDF-PLGA-SS-PEG micelles with conjugate concentration of 100 μg/ml.

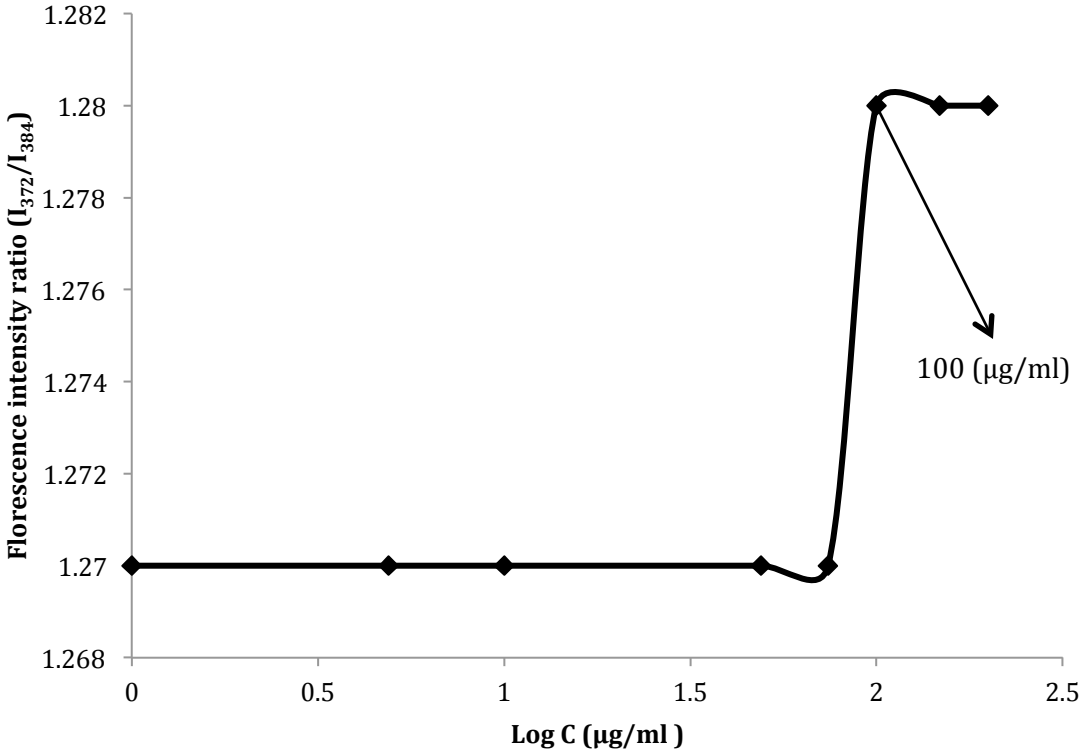

Figure 10: CMC for PLGA-SS-PEG micelles using pyrene as a fluorescence probe.

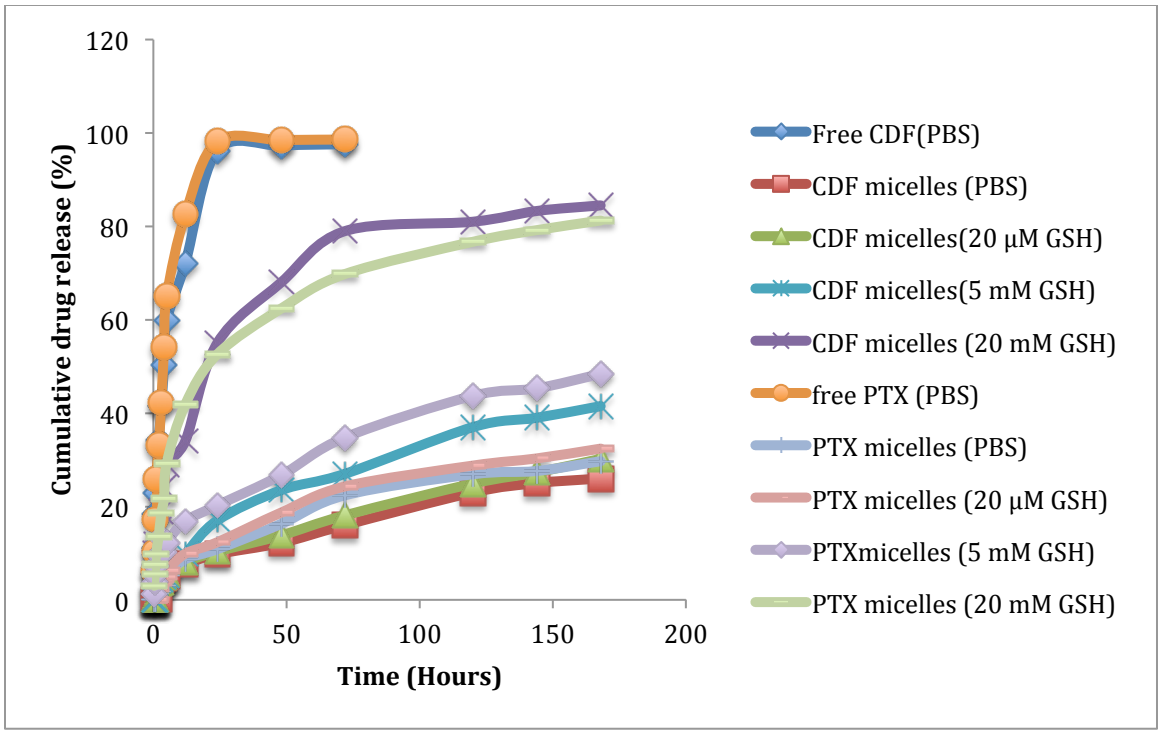

Figure 11: Invitro drug release studies of micelle coencapsulating CDF and paclitaxel in PBS and PBS containing 20 µM, 20 mM and 5 mM GSH.

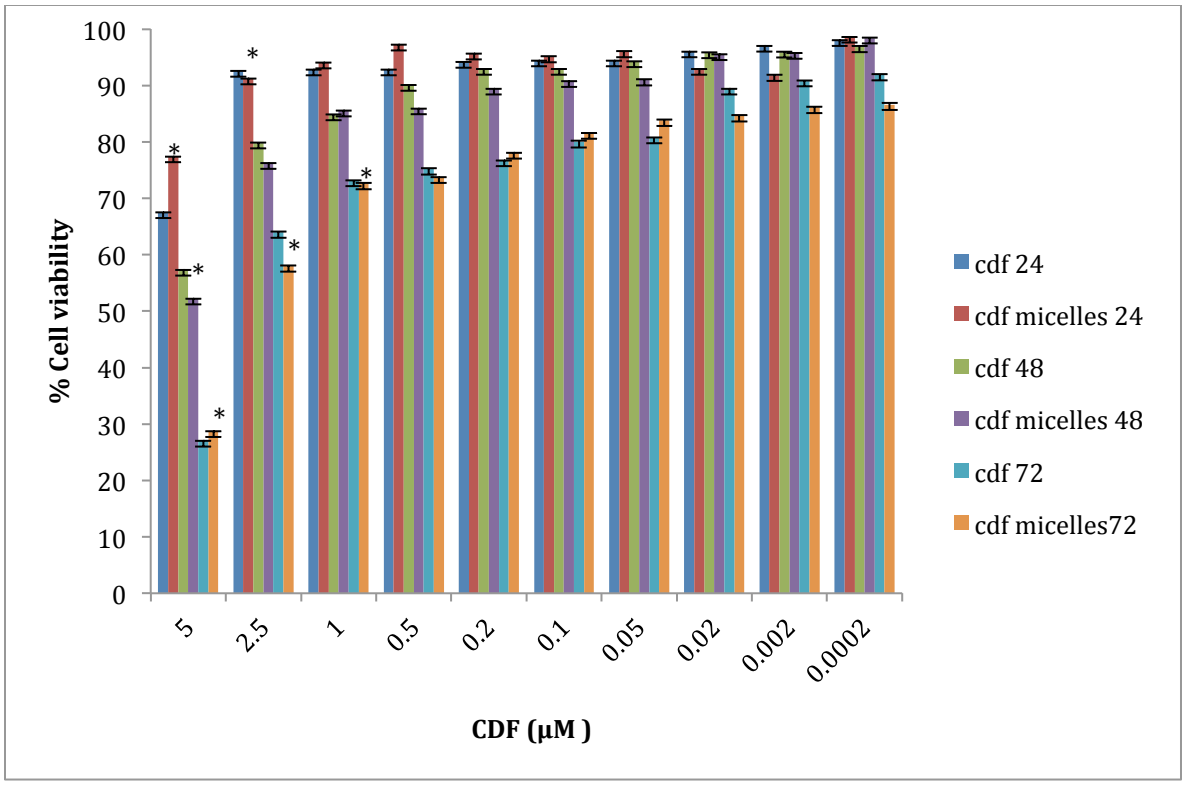

Figure 12: Percentage Cell viability of BXPC3 cells upon incubation with free CDF and micelles encapsulating CDF at the end of 24 h, 48 h and 72 h; *, $p<0.05$ between drug and micelles (n=8; mean ± S.D)

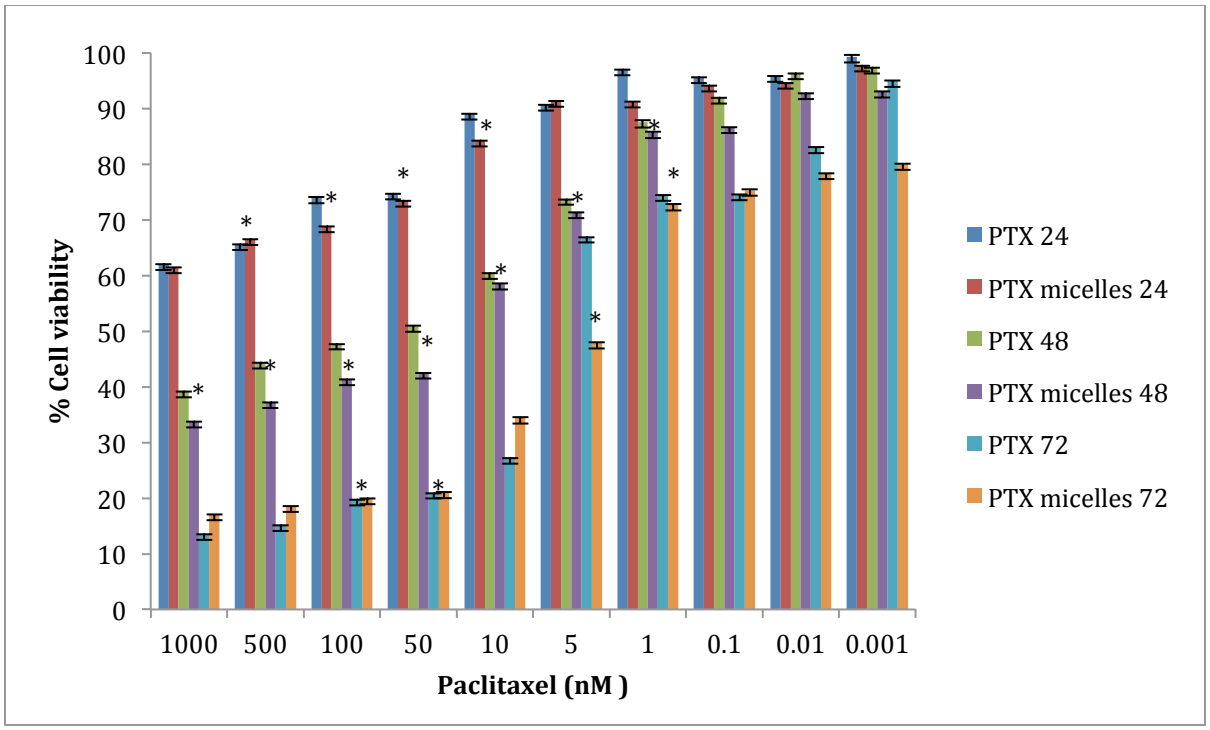

Figure 13: Percentage Cell viability of BXPC3 cells upon incubation with free Paclitaxel and micelles encapsulating Paclitaxel at the end of 24 h, 48 h and 72 h; *, $p<0.05$ between drug and micelles (n=8; mean ± S.D)

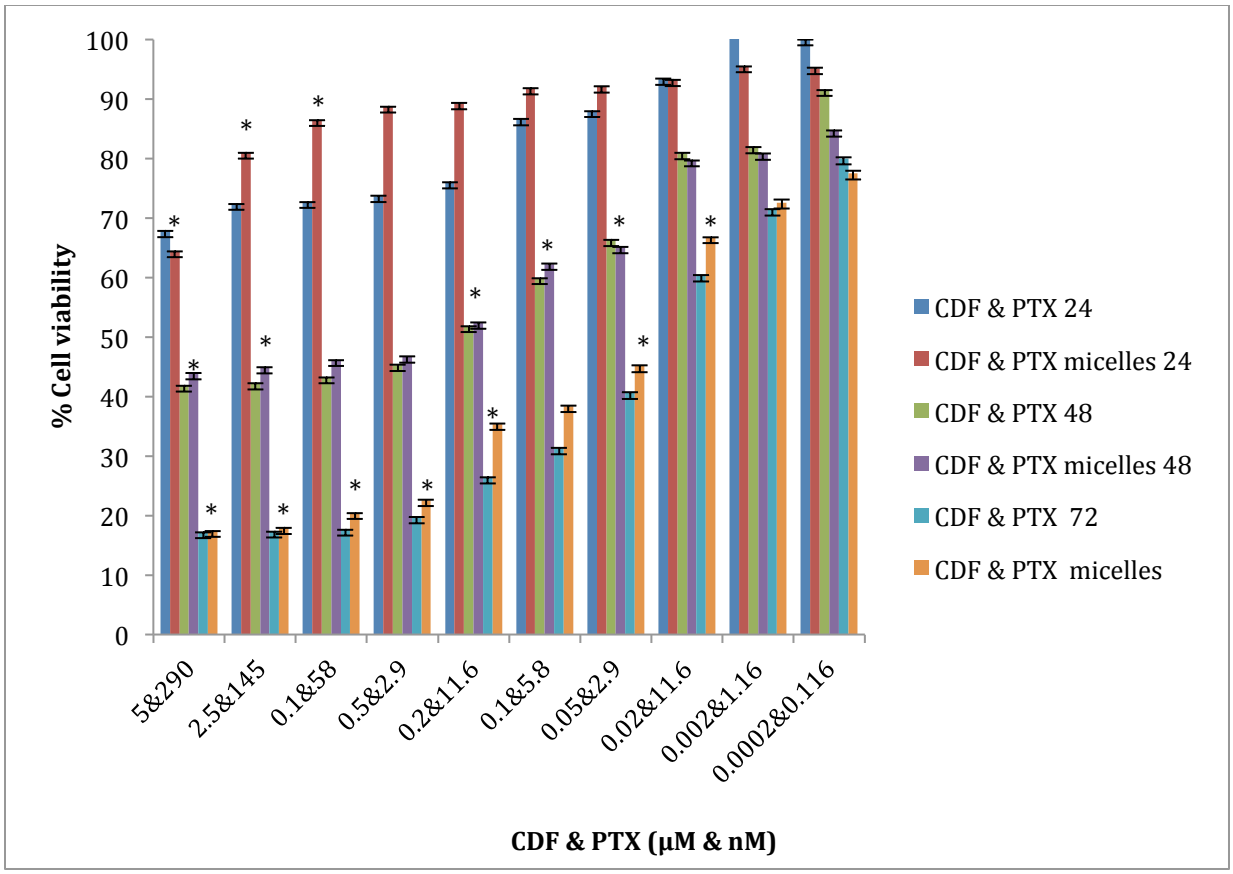

Figure 14: Percentage Cell Cell viability of BXPC3 cells upon incubation with free CDF and Paclitaxel and micelles encapsulating both CDF & Paclitaxel at the end of 24 h, 48 h and 72 h; *, $p<0.05$ between drug and micelles (n=8; mean ± S.D)

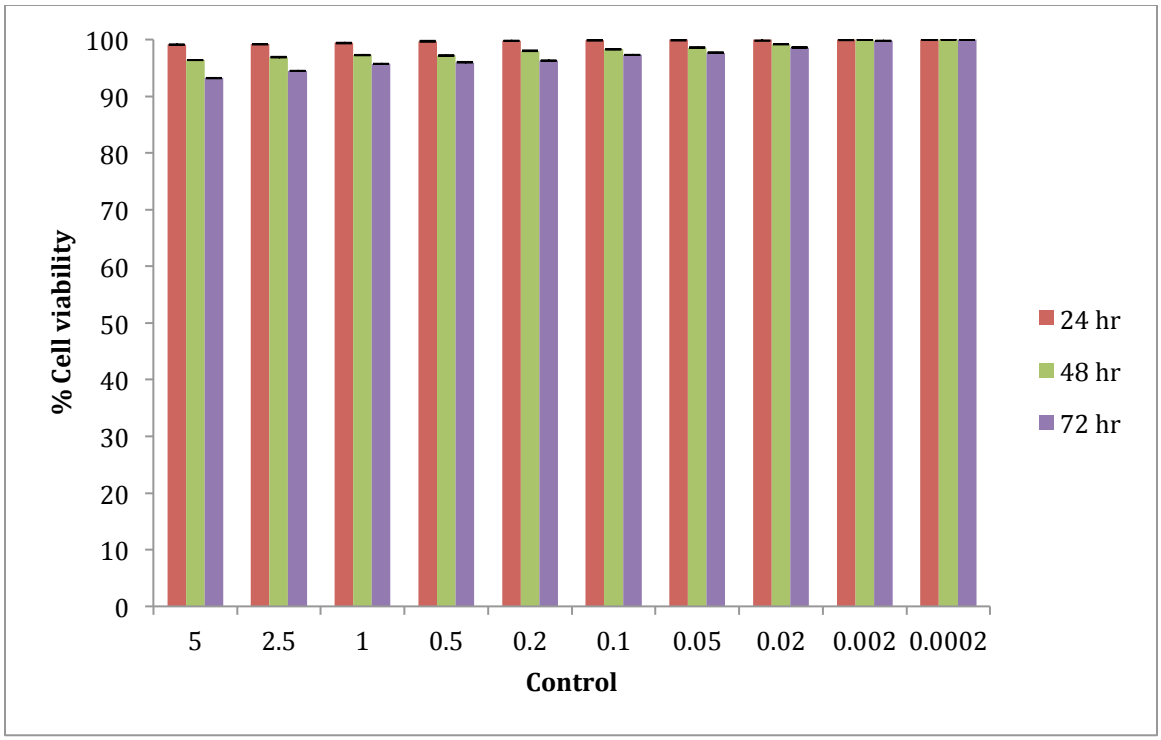

Figure 15: Percentage Cell Cell viability of BXPC3 cells upon incubation with control micelles at the same dilutions as micelles with drug at the end of 24 h, 48 h and 72 h. (n=8; mean ± S.D)

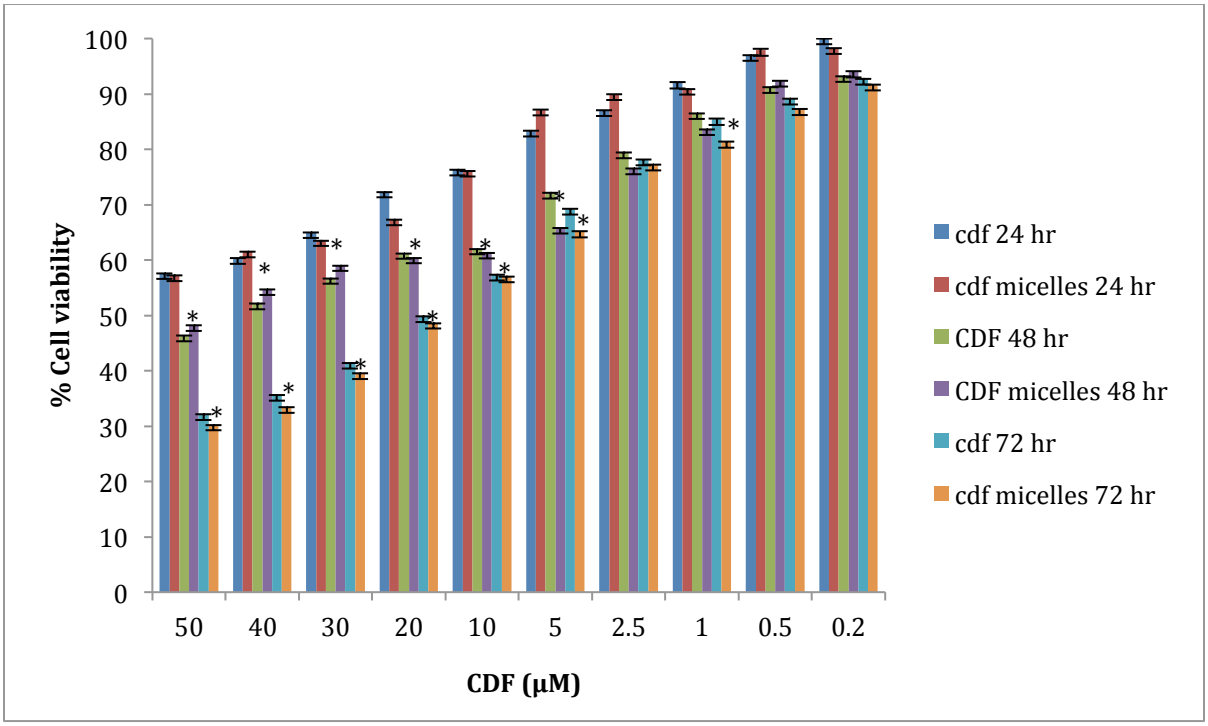

Figure 16: Percentage Cell Cell viability of SKOV3 cells upon incubation with free CDF and micelles encapsulating CDF at the end of 24 h, 48 h and 72 h; *, $p<0.05$ between drug and micelles (n=8; mean ± S.D)

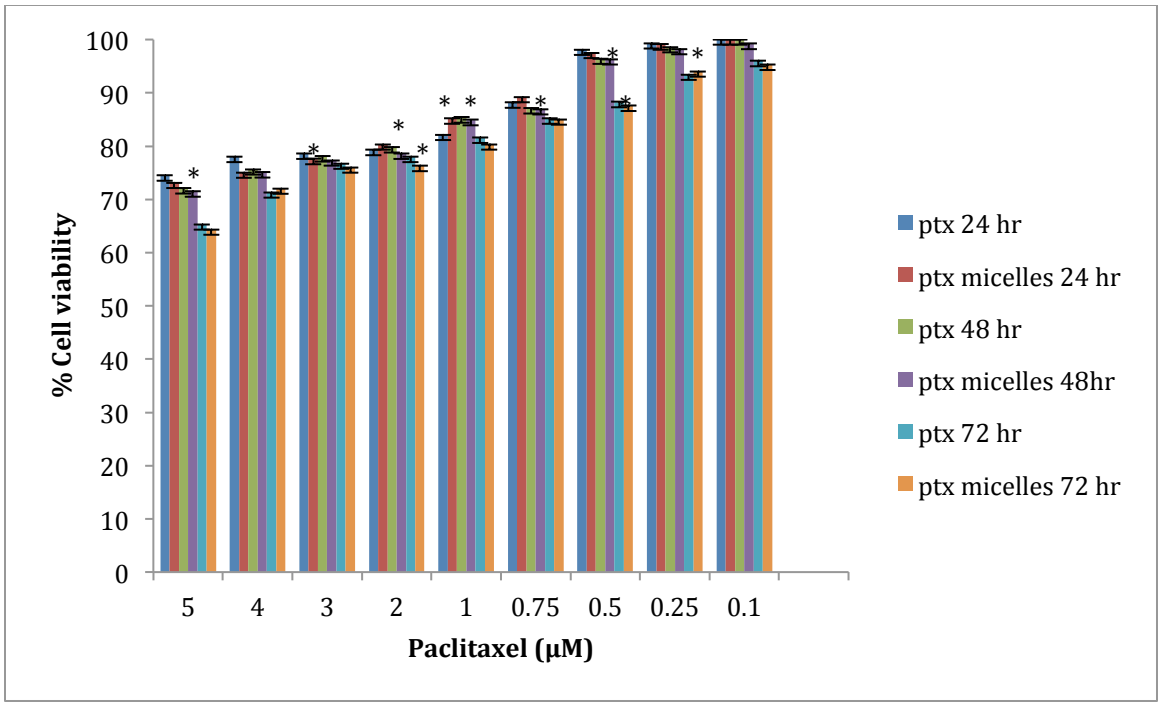

Figure 17: Percentage Cell Cell viability of SKOV3 cells upon incubation with free Paclitaxel and micelles encapsulating Paclitaxel at the end of 24 h, 48 h and 72 h; *, $p<0.05$ between drug and micelles (n=8; mean ± S.D)

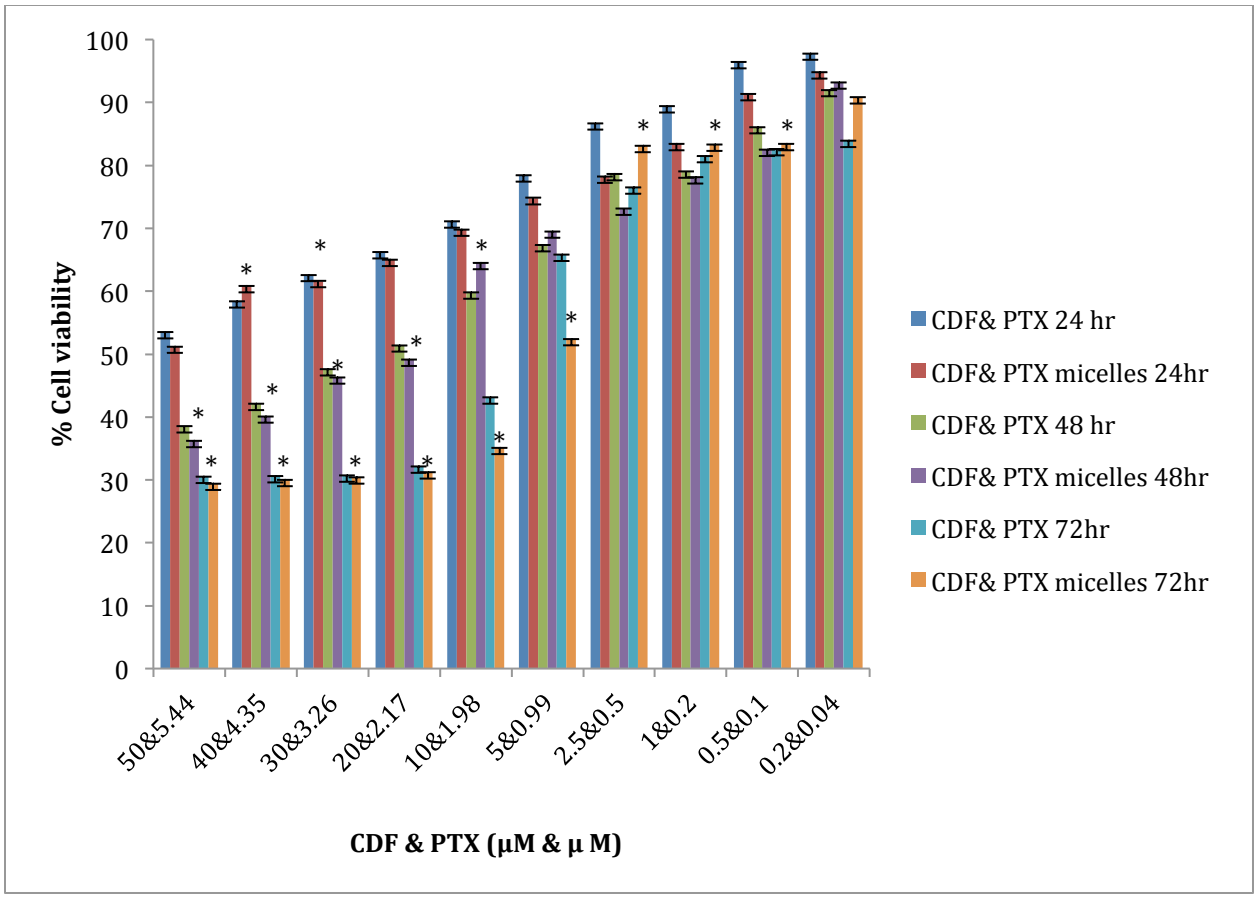

Figure 18: Percentage Cell Cell viability of SKOV3 cells upon incubation with free CDF and paclitaxel and micelles encapsulating both CDF & Paclitaxel at the end of 24 h, 48 h and 72 h; *, $p<0.05$ between drug and micelles (n=8; mean ± S.D)

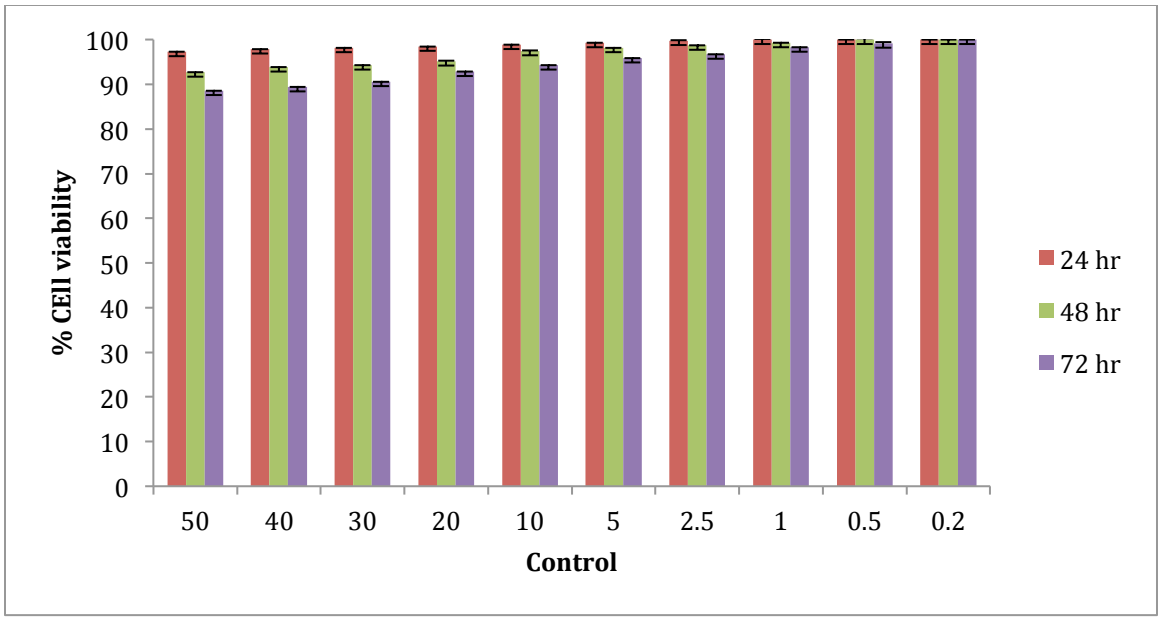

Figure 19: Percentage Cell Cell viability of SKOV3 cells upon incubation with control micelles at the same dilutions as micelles with drug at the end of 24 h, 48 h and 72 h. (n=8; mean ± S.D)

Time (Hours)	Free CDF (μM)	Free Paclitaxel (nM)	Free CDF & Paclitaxel (μM & nM)	PLGA-SS-PEG micelles encapsulating CDF (μM)	PLGA-SS-PEG micelles encapsulating Paclitaxel (nM)	PLGA-SS-PEG micelles coencapsulating CDF & Paclitaxel (μM & nM)
24	12.9	527	4.8 & 281.5	15.3	610.4	5.3 & 308
48	5.9	45.82	0.79 & 34.54	6.76	33.46	0.48 & 28.3
72	2.4	10.4	0.15 & 7.5	2.1	9.82	0.13& 6.4

Table 4: IC50 values of CDF and paclitaxel alone and in combination on BXPC3 cells, in the free drug form and micelle formulation

Time (Hours)	Free CDF (μM)	Free Paclitaxel (μM)	Free CDF & free Paclitaxel (μM & μM)	PLGA-SS-PEG micelles encapsulating CDF (μM)	PLGA-SS-PEG micelles encapsulating Paclitaxel (μM)	PLGA-SS-PEG micelles coencapsulating CDF & Paclitaxel (μM & μM)
24	51.3	11.32	42.12 & 3.44	49.68	10.78	39.2 & 3.27
48	29.44	10.59	19.48 & 2.12	29.79	10.15	18.68 & 2.09
72	16.37	8.22	9.8 &1.56	14.7	7.9	8.2 & 1.48

Table 5: IC50 values of CDF and paclitaxel alone and in combination on SKOV3 cells, in the free drug form and micelle formulation

Time points (Hours)	Free drug combination	Micelles formulations
24	1	0.99
48	0.7	0.65
72	0.66	0.62

Table 6: CDF and paclitaxel combination index (CI) against SKOV3 cells CI < 1, synergistic; CI = 1, additive; CI > 1, antagonistic.

Time points (Hours)	Free drug combination	Micelles formulations
24	0.9	0.85
48	0.88	0.87
72	0.77	0.7

Table 7: CDF and paclitaxel combination index (CI) against BXPC3 cells CI < 1, synergistic; CI = 1, additive; CI > 1, antagonistic.

Drug	BXPC 3	SKOV 3
CDF	16	1.7
Paclitaxel	1.5	5.3

Table 8: Dose reduction index (DRI) values for CDF and paclitaxel with micelles coencapsulating both CDF and paclitaxel when compared to CDF micelles and paclitaxel micelles in BXPC3 and SKOV3 cell lines at 72 h time point.

CHAPTER 5: CONCLUSIONS AND FUTURE DIRECTIONS

The design, synthesis, characterization and invitro evaluation of CDF-PLGA-S-S-PEG micelles encapsulating CDF, paclitaxel and both were investigated here are representation of nanocarriers which have the ability to improve the solubility of the free drug. Favorable size distribution, very low CMC, good biocompatibility of prepared micelles proved their greater potential for delivering anti cancer drugs via intravenous injection in the cancer treatment. The prepared copolymer has self-assembled properties which was confirmed by its low CMC (100 µg/ml). The nanomicelles were successfully prepared with drug loading capacity of around 9% for all the formulations. But the conjugated CDF loading was very less 0.4%. The prepared conjugate was successful in encapsulating CDF and paclitaxel individually and also as combined formulation. The drug release studies proved that these micelles displayed low drug release under non-reductive environment while releasing the drug rapidly and quantitatively in presence varying concentrations of reducing agent GSH.

In both the cell lines there was a clear time and concentration dependent cell growth inhibition was observed. In case of SKOV3 and BXPC3 cell lines, the IC50 values were very close to free drug indicating the encapsulation of free drugs in to micelles did not hamper their

therapeutic properties. The micelles encapsulating both CDF and paclitaxel were found to be much more efficient than when individual drugs were incorporated in both the cell lines. The IC50 of both the drugs reduced when used in combination and CDF proved to sensitize the SKOV3 cells to paclitaxel therapy.

The present study indicates that the co-delivery system provides a promising platform for cancer therapy as the combination treatment is much efficient in multi drug resistant cancers. Since the IC50 of drugs can be reduced when used in combination, the overall side effects of these drugs can be reduced by decreasing the dose of the drug given to the patient. By using PLGA-S-S-PEG micelles, it is possible to incorporate multiple drugs in one formulation along with smaller size of micelles, disulfide bond which can breakdown only in presence of highly reductive environment like tumor cells and PEG outer layer which prevents the uptake by MPS system, these micelles can circulate longer time in plasma and because of EPR effect they can successfully reach tumor cells without releasing the drug any where else in the body.

In summary, our work of fabricating polymeric micelles coencapsulating two drugs has significant implications in treatment of various multi drug resistant cancers. This body of work provides a platform

for developing micelle systems with different drugs to treat various cancers. Specifically, results from this work will be used in the future to investigate the synergistic therapeutic effect in pancreatic and ovarian cancer mice model. Finally, based on the knowledge gained from all my work, polymeric micelles could provide a platform for an effective drug delivery system which can be passively and actively target the tumor site along with multi drug delivery to the tumor.

REFERENCES

1. Clifford J. Whatcott, R.G.P., Daniel D. Von Hoff, and Haiyong Han, *Desmoplasia and chemoresistance in pancreatic cancer*. Pancreatic cancer and tumor microenvironment. 2012: Transworld Research Network.
2. Szakács G, P.J., Ludwig JA, Booth-Genthe C, Gottesman MM, *Targeting multidrug resistance in cancer.* Nat Rev Drug Discov, 2006. **5**(3): p. 219-234.
3. Jemal, A., et al., *Cancer statistics, 2009.* CA Cancer J Clin, 2009. **59**(4): p. 225-49.
4. http://training.seer.cancer.gov/disease/cancer/, *SEER Training Modules, Cancer as a disease.* U. S. National Institutes of Health, National Cancer Institute., 01/05/2014.
5. *<Cell Biology and Cancer.pdf>.*
6. *world cancer report 2008*.
7. Ghaneh, P., E. Costello, and J.P. Neoptolemos, *Biology and management of pancreatic cancer.* Postgraduate Medical Journal, 2008. **84**(995): p. 478-497.
8. Pandol, S., et al., *Desmoplasia of pancreatic ductal adenocarcinoma.* Clin Gastroenterol Hepatol, 2009. **7**(11 Suppl): p. S44-7.
9. Shimizu, K., *Mechanisms of pancreatic fibrosis and applications to the treatment of chronic pancreatitis.* Journal of Gastroenterology, 2008. **43**(11): p. 823-832.
10. loos, M., et al, *Surgical treatment of pancreatic cancer.* Ann N Y Acad Sci, 2008(1138): p. 169-180.
11. Wagner, M., et al, *Curative resection is the single most important factor determining outcome in patients with pancreatic adenocarcinoma.* British Journal of Surgery, 2004. **91**(5): p. 586-594.

12. Zalatnai, A.a.J.M., *Review. Molecular background of chemoresistance in pancreatic cancer. In vivo.* 2007. **21**(3): p. 339-347.

13. Kim, M.P.a.G.E.G., *Gemcitabine resistance in pancreatic cancer: picking the key players.* clinical cancer research, 2007. **14**(5): p. 1284-1285.

14. sakai, W., et al, *Secondary mutations as a mechanism of cisplatin resistance in BRCA2-mutated cancers.* nature, 2008. **451**(7182): p. 1116-1120.

15. B, B., *plants consumed by man.* newyork, acdemic press

, 1975: p. 331.

16. Goel, A. and B.B. Aggarwal, *Curcumin, the golden spice from Indian saffron, is a chemosensitizer and radiosensitizer for tumors and chemoprotector and radioprotector for normal organs.* Nutr Cancer, 2010. **62**(7): p. 919-30.

17. Sharma, R.A., A.J. Gescher, and W.P. Steward, *Curcumin: the story so far.* Eur J Cancer, 2005. **41**(13): p. 1955-68.

18. Teiten, M.H., et al., *Curcumin-the paradigm of a multi-target natural compound with applications in cancer prevention and treatment.* Toxins (Basel), 2010. **2**(1): p. 128-62.

19. Lin, j.-K., *Molecular targets of curcumin.* ADVANCES IN EXPERIMENTAL MEDICINE AND BIOLOGY 2007. **595**: p. 227-243.

20. H, B.I.a.O., *Curcumin, an anti-tumour promoter and anti- inflammatory agent, inhibits induction of nitric oxide synthase in activated macrophages.* biochemical and biophysical research communications, 1995. **206**: p. 533-540.

21. MN, S.x.R., *Nitric oxide scavenging by curcuminoids.* journal of pharmacy and pharmacology, 1997. **49**: p. 105-107.

22. MR, D.C.a.P., *Antitumor action of curcumin in human pa- pillomavirus associated cells involves downregulation of viral oncogenes, prevention of NFkB and AP-1 translocation, and modulation of apoptosis.* molecular carcinogenesis, 2006. **45**: p. 320-332.

23. Kiso Y , S.Y., Watanabe N, Oshima Y , and Hikino H, *Antihepatotoxic principles of Curcuma longa rhizomes.* planta medica, 1983. **49**: p. 185-187.

24. Srivastava R, D.M., Srimal RC, and Dhawan BN, *Anti-thrombotic effect of curcumin.* thrombosis research, 1985. **40**: p. 413-417.

25. N, V., *Curcumin attenuation of acute adriamycin myocardial toxi- city in rats.* british journal of pharmacology, 1998. **124**: p. 425-427.

26. Deodhar SD, S.R., and Srimal RC, *Preliminary study on antirheumatic activity of curcumin (diferuloyl methane).* Indian journal of medical research, 1980. **71**: p. 631-634.

27. Chan MM, A.N., and Fong D, *Curcumin overcomes the inhibitory effect of nitric oxide on Leishmania.* Parasitology research, 2005. **96**: p. 49-56.

28. Cheng AL, H.C., Lin JK, et al, *Phase I clinical trial of curcumin, a chemopreventive agent, in patients with high-risk or pre-malignant lesions.* Anticancer research, 2001. **21**: p. 2895-2900.

29. Aggarwal BB, K.A., Bharti AC, *Anticancer potential of curcumin: preclinical and clinical studies.* Anticancer research, 2003. **23**: p. 363-398.

30. Rajesh L. Thangapazham, A.S.a.R.K.M., *Multiple molecuar targets in cancer chemoprevention by curcumin.* The AAPS Journal, 2006. **8**(3).

31. Fazlul H. Sarkar, Q.P.D., Subhash Padhye, *Novel analogs of curcumin and methods of use*. 2011.

32. Jutooru, I., et al., *Inhibition of NFkappaB and pancreatic cancer cell and tumor growth by curcumin is dependent on specificity protein down-regulation.* J Biol Chem, 2010. **285**(33): p. 25332-44.

33. Holcomb B, Y.-S.M., Matos JM, Dixon J, Kennard J, et al, *Pancreatic cancer cell genetics and signaling response to treatment corre- late with efficacy of gemcitabine-based molecular targeting strategies.* J Gastrointest Surg 2008. **12**: p. 288-296.

34. Hour TC, C.J., Huang CY, Guan JY, Lu SH, et al, *Curcumin enhances cytotoxicity of chemotherapeutic agents in prostate cancer cells by inducing p21(WAF1/CIP1) and C/EBPbeta expressions and suppressing NF-kappaB activation.* Prostate, 2002. **51**: p. 211-218.

35. Chan MM, F.D., Soprano KJ, Holmes WF, and Heverling H, *Inhibition of growth and sensitization to cisplatin-mediated killing of ovarian cancer cells by polyphenolic chemopreventive agents.* J Cell Physiol, 2003. **194**: p. 63-70.

36. Navneet Dhillon, B.B.A., Robert A. Newman, et al, *Phase II Trial of Curcumin in Patients with Advanced Pancreatic Cancer.* Clin Cancer Res 2008. **14**: p. 4491-4499.

37. Takahashi, M., et al, *Characterization and bioavailability of liposomes containing a ukon extract.* Biosci Biotechnol Biochem, 2008. **72**(5): p. 1199-1205.

38. Maiti, K., et al, *Curcumin-phospholipid complex: Preparation, therapeutic evaluation and pharmacokinetic study in rats.* Int J Pharm, 2007. **330**(1-2): p. 155-163.

39. Ma, Z., et al, *High-performance liquid chromatography analysis of curcumin in rat plasma: application to pharmacokinetics of polymeric micellar formulation of curcumin.* Biomed Chromatogr, 2007. **21**(5): p. 546-552.

40. Bisht, S., et al, *Polymeric nanoparticle-encapsulated curcumin ("nanocurcumin"): a novel strategy for human cancer therapy.* J Nanobiotechnology, 2007. **5**: p. 3.

41. Anand, P., et al, *Design of curcumin-loaded PLGA nanoparticles formulation with enhanced cellular uptake, and increased bioactivity in vitro and superior bioavailability in vivo.* Biochem Pharmacol, 2010. **79**(3): p. 330-338.

42. Yallapu, M.M., M. Jaggi, and S.C. Chauhan, *beta-Cyclodextrin-curcumin self-assembly enhances curcumin delivery in prostate cancer cells.* Colloids Surf B Biointerfaces. **79**(1): p. 113-125.

43. Shahani, K., et al, *Injectable sustained release microparticles of curcumin: a new concept for cancer chemoprevention.* Cancer Res, 2010. **70**(11): p. 4443-4452.

44. Gou, M., et al., *Curcumin-loaded biodegradable polymeric micelles for colon cancer therapy in vitro and in vivo.* Nanoscale, 2011. **3**(4): p. 1558-67.

45. Yallapu, M.M., et al, *Fabrication of curcumin encapsulated PLGA nanoparticles for improved therapeutic effects in metastatic cancer cells.* Journal of Colloid and Interfacial Science, 2010. **351**(1): p. 19-29.

46. Shaikh, J., et al, *Nanoparticle encapsulation improves oral bioavailability of curcumin by at least 9-fold when compared to curcumin administered with piperine as absorption enhancer.* Eur J Pharm Sci, 2009. **37**(3-4): p. 223-230.

47. Zambare AP, J.A., Padhye S, Kulkarni VM, *Copper conjugates of Knoevenagel condesates of Curcumin and their Schiff base derivatives: synthesis, spectroscopy,*

magnetism, EPR and electrochemistry. Synth React Inorg, Metal-Org and NanoMetal Chemistry, 2007. **37**(19-27).

48. Padhye, S., et al., *New difluoro Knoevenagel condensates of curcumin, their Schiff bases and copper complexes as proteasome inhibitors and apoptosis inducers in cancer cells.* Pharm Res, 2009. **26**(8): p. 1874-80.

49. Padhye, S., et al., *Fluorocurcumins as cyclooxygenase-2 inhibitor: molecular docking, pharmacokinetics and tissue distribution in mice.* Pharm Res, 2009. **26**(11): p. 2438-45.

50. Ali, S., et al., *Gemcitabine sensitivity can be induced in pancreatic cancer cells through modulation of miR-200 and miR-21 expression by curcumin or its analogue CDF.* Cancer Res, 2010. **70**(9): p. 3606-17.

51. Bin Bao, S.A., Dejuan Kong, Sanila H. Sarkar, Zhiwei Wang, Sanjeev Banerjee, Amro Aboukameel, Subhash Padhye, Philip A. Philip, Fazlul H. Sarkar, *Anti-Tumor Activity of Novel Compound-CDF Is Mediated by Regulating mir-21, mir-200, and PTEN in Pancreatic Cancer.* PLos ONE, 2011. **6**(3): p.

.

52. Padhye, S., et al, *New difluoro Knoevenagel condensates of curcumin, their Schiff bases and copper*

complexes as proteasome inhibitors and apoptosis inducers in cancer cells. Pharmaceutical Research, 2009. **26**(8): p. 1874-80.

53. Dandawate, P.R., et al., *Inclusion complex of novel curcumin analogue CDF and beta-cyclodextrin (1:2) and its enhanced in vivo anticancer activity against pancreatic cancer.* Pharm Res, 2012. **29**(7): p. 1775-86.

54. Sutton, D., et al., *Functionalized micellar systems for cancer targeted drug delivery.* Pharm Res, 2007. **24**(6): p. 1029-46.

55. Yokoyama, M., *Clinical Applications of Polymeric Micelle Carrier Systems in Chemotherapy and Image Diagnosis of Solid Tumors.* Journal of Experimental & Clinical Medicine, 2011. **3**(4): p. 151-158.

56. Loh, W., *BLOCK COPOLYMER MICELLES.* Encyclopedia of Surface and Colloid Science, 2002.

57. Riess, G., *Micellization of block copolymers.* Progress in Polymer Science, 2003. **28**(7): p. 1107-1170.

58. Yokoyama, M., *Supramolecular Design for Biological Applications*. Drug targeting with polymeric micelles drug carriers. 2002: CRC Press.

59. Sezgin, Z., N. Yuksel, and T. Baykara, *Preparation and characterization of polymeric micelles for solubilization of poorly soluble anticancer drugs.* Eur J Pharm Biopharm, 2006. **64**(3): p. 261-8.

60. Kataoka Kazunori, K.G.S., Yokoyama Masayuki, Okano Teruo, Sakurai Yasuhisa, *Block copolymer micelles as vehicles for drug delivery.* Journal of Controlled Release, 1993. **24**(1-3): p. 119-132.

61. Chris Oerlemans , W.B.M.B., Gert Storm,J. Frank W. Nijsen, Wim E. Hennink, *Polymeric Micelles in Anticancer Therapy: Targeting, Imaging and Triggered Release.* Pharm Res, 2010. **27**: p. 2569-2589.

62. Brannon-Peppas, L. and J.O. Blanchette, *Nanoparticle and targeted systems for cancer therapy.* Advanced Drug Delivery Reviews, 2012. **64**: p. 206-212.

63. Orr, G.A., et al., *Mechanisms of Taxol resistance related to microtubules.* Oncogene, 2003. **22**(47): p. 7280-95.

64. A Stierle, G.S., D Stierle, *Taxol and taxane production by Taxomyces andreanae, an endophytic fungus of Pacific yew.* science, 1993. **260**: p. 214-216.

65. K, P., *Paclitaxel Against Cancer: A Short Review.* Medicinal chemistry, 2012. **02**(07).

66. *cancer drug information Paclitaxel*, N.c. institute, Editor. 2006.

67. *Paclitaxel*. Available from: http://ncit.nci.nih.gov/ncitbrowser/ConceptReport.jsp?dictionary=NCI_Thesaurus&code=C1411&ns=NCI_Thesaurus.

68. Park S, K.S., Chen X, Kim EJ, Kim J, Kim N, Kim J, Jin MM, *Tumor suppression via paclitaxel-loaded drug carriers that target inflammation marker upregulated in tumor vasculature and macrophages.* BIomaterials, 2013. **34**(2): p. 598-605.

69. Jianan Shena, H.S.b., Pengfei Xua, Qi Yina, Zhiwen Zhanga, Siling Wangb, Haijun Yua, Yaping Lia, *Simultaneous inhibition of metastasis and growth of breast cancer by co-delivery of twist shRNA and paclitaxel using pluronic P85-PEI/TPGS complex nanoparticles.* Biomaterials, 2013. **34**(5): p. 1581-1590.

70. Byron SA, L.D., Pollock PM, *Fibroblast growth factor receptor inhibition synergizes with Paclitaxel and Doxorubicin in endometrial cancer cells.* Int J Gynecol Cancer, 2012. **22**(9): p. 1517-1526.

71. T. Huang, W.H.G., X. C. Li, C. P. Zou, G. J. Jiang, X. H. Li, D. P. Feng, *Synergistic increase in the sensitivity of osteosarcoma cells to thermochemotherapy with combination of paclitaxel and etoposide.* Molecular medicine reports, 2012. **6**: p. 1013-1017.

72. Yang JC, L.M., Lee CL, Chen GY, Lin YY, Chang FR, Wu YC, *Selective targeting of breast cancer cells through ROS-mediated mechanisms potentiates the lethality of paclitaxel by a novel diterpene, gelomulide K.* Free Radic Biol Med, 2011. **51**(3): p. 647-657.

73. H. Gelderblom*, J.V., K. Nooter, A. Sparreboom, *Cremophor EL: the drawbacks and advantages of vehicle selection for drug formulation.* European Journal of Cancer, 2001. **37**: p. 1590-1598.

74. *<Nanocarriers as an emerging platform for cancer therapy.pdf>.*

75. Bellamy WT, D.W., *Multidrug resistance in the laboratory and clinic.* Adv Clin Chem, 1994. **31**: p. 1-61.

76. Limtrakul, P., Chearwae, W, Shukla, S, Phisalphong, C, Ambudkar, S. V, *Modulation of function of three ABC drug transporters, P-glycoprotein (ABCB1), mitoxantrone resistance protein (ABCG2) and multidrug resistance protein 1 (ABCC1) by tetrahydrocurcumin, a major metabolite of curcumin.* Mol. Cell. Biochem, 2007. **296**(1): p. 85-95.

77. Amiji, S.G.a.M., *Coadministration of Paclitaxel and Curcumin in Nanoemulsion Formulations To Overcome Multidrug Resistance in Tumor Cells.* mol.Pharmaceutics, 2009. **6**(3): p. 928-939.

78. Mohsen Ashjari, S.K., Ali Reza Mahdavian, Reza Rahmatolahzadeh, *Self-assembled nanomicelles using PLGA–PEG amphiphilic block copolymer for insulin delivery: a physicochemical investigation and determination of CMC values.* J Mater Sci: Mater Med 2012. **23**: p. 943-953.

79. Ana Domínguez, A.F.n., Noemí González, Emilia Iglesias, Luis Montenegro, *Determination of Critical Micelle Concentration of Some Surfactants by Three Techniques.* Journal of Chemical Education, 1997. **74**(10).

80. Chou, T.C., *Drug combination studies and their synergy quantification using the Chou-Talalay method.* Cancer Res, 2010. **70**(2): p. 440-6.

81. Chou, T.C., *Theoretical basis, experimental design, and computerized simulation of synergism and antagonism in drug combination studies.* Pharmacol Rev, 2006. **58**(3): p. 621-81.

82. Ren, T.-B., et al., *Sheddable micelles based on disulfide-linked hybrid PEG-polypeptide copolymer for intracellular drug delivery.* Polymer, 2011. **52**(16): p. 3580-3586.

83. Verma, A. and F. Stellacci, *Effect of surface properties on nanoparticle-cell interactions.* Small, 2010. **6**(1): p. 12-21.

84. Li, J., et al., *Redox-sensitive micelles self-assembled from amphiphilic hyaluronic acid-deoxycholic acid conjugates for targeted intracellular delivery of paclitaxel.* Biomaterials, 2012. **33**(7): p. 2310-20.

85. Wang, K., et al., *Novel shell-cross-linked micelles with detachable PEG corona for glutathione-mediated intracellular drug delivery.* Soft Matter, 2013. **9**(3): p. 692.

ABSTRACT

DEVELOPMENT AND EVALUATION OF PLGA-S-S-PEG MICELLES COENCAPSULATING CURCUMIN DIFLUORINATED AND PACLITAXEL FOR SYNERGISTIC THERAPEUTIC EFFICACY

by

LAKSHMI DEEPIKA CHEEMALAKONDA

August 2014

Advisor: Dr. Joshua Reineke

Major: Pharmaceutical Sciences

Degree: Master of Science

Solid tumors like pancreatic tumor has unique property of forming a dense desmoplastic layer around the tumor cells making it difficult for the drug to transport across this layer. Multi drug resistance is also one of the major limitation of chemotherapy. Therefore the aim of this project was to make PLGA-SS-PEG micelles encapsulating CDF and paclitaxel for synergistic cancer therapy. CDF was found to have 16-fold better half-life when compared to curcumin maintaining equivalent bioactivity. Since CDF has chemosensitizing property we tested this by incorporating CDF and paclitaxel in same formulation and tested their synergy on BXPC3 pancreatic cancer cell line and SKOV3 ovarian cancer cell line that is paclitaxel resistant. Here we utilized a number of techniques including

incorporation of PEG surface molecules thereby avoiding uptake by monophagocytic system and cysteine protease liable conjugation of PEG to the micelles making CDF and paclitaxel release specific to tumor tissue by enhanced permeation and retention effect. All the micelle formulations were below 200 nm size range. Our drug release study proved that these micelles undergo a fast sheddable process upon encountering the reduction sensitive condition like higher glutathione (GSH) levels. Cell cytotoxicity studies revealed the copolymer has good biocompatibility and self-assembled micelles showed drug loading of around 9 % for both the drugs and they released the drug quantitatively in response to the level of GSH. The synergistic effect was studied by Chou-Talalay method. There was a time and concentration dependent cell killing. Maximum synergy was observed at 72 h time point for BXPC3 cells and SKOV3 cells at 72 h time point with PLGA-S-S-PEG micelles coencapsulating both CDF and paclitaxel. The micelle formulation has higher synergy than compared to free drug combination in both cell lines at 72 hour time point. Overall IC50 values of both CDF and paclitaxel were reduced when used in combination. Based on the results of our study it indicates that these micelles have a potential promote tumor penetration because of smaller size, prolonged circulation and EPR effect and release the drug specifically in tumor cells

upon exposure to highly reductive environment. Since these micelles incorporated two drugs they will be efficient for chemotherapy in multi drug resistant tumors.

AUTOBIOGRAPHICAL STATEMENT

EDUCATION

- M.S Pharmaceutical sciences, August 2014, Wayne state university, Detroit, MI.
- Masters of Pharmacy (Pharmaceutics), September 2007, Rajiv Gandhi University of Health Sciences, Bangalore, India
- Bachelors of Pharmacy, September 2004, Rajiv Gandhi University of Health Sciences, Bangalore, India